



Ph.D. Dissertation

Glass Particles as an Active and CO₂ Reducing Component in Future Cement

by
Mette Moesgaard

Section of Chemistry
Department of Biotechnology, Chemistry and
Environmental Engineering
Aalborg University

Date of defense
10.12.2010

Assessment committee
Reinhard Conradt
Department of Glass and Ceramic
Composites
RWTH Aachen University, Germany
Donald E. MacPhee
Mechanics of Materials Research Group
University of Aberdeen, Scotland
Kristian Keiding
Aalborg University

Supervisor
Yuanzheng Yue
Aalborg University

Abstract

Portland cement manufacture is an energy intensive industry responsible for approximately 5% of the global anthropogenic CO₂ emission. Considerable efforts are thus being made by the industries to reduce their CO₂ emissions.

The approach taken in this study is to lower the CO₂ emissions from cement production by clinker substitution. This means that the clinker is partly substituted by supplementary cementitious materials (SCMs). This work deals with the development of innovative SCMs based on calcium aluminosilicate (CAS) glass particles produced specifically for the purpose as SCM. The objectives of this study fall into two parts: 1) Optimization of the composition of the CAS glasses to reduce the CO₂ emission linked to glass production while at the same time ensuring high pozzolanic reactivity (i.e., the ability of the glasses to participate in the formation of strength giving hydration phases when mixed with the cement); 2) Study of both the physical performances of blended cements containing 30 wt% of the newly developed SCMs and the hydration behavior. In addition to the blended cements containing just one SCM, investigations are carried out on cements containing both limestone and CAS glass particles.

It is found that one tonne of the CAS glasses made from natural raw materials namely clay, limestone and sand, referred to as the so-called CLS glasses, can be produced emitting less than 60% of the CO₂ released producing one tonne of clinker. In addition, the glasses possess pozzolanic reactivity upon contact with water and Ca(OH)₂ forming hydration products resembling the C-S-H and the calcium aluminate hydration phases formed during Portland cement hydration.

Investigations of the composition-structure relationship of a range of three components CAS model glasses show evidence of structural heterogeneity to exist in the intermediate-range order. This is manifested as clustering of highly depolymerized regions with only limited Al present and highly polymerized regions of alternating SiO₄ and AlO₄ tetrahedra.

Examinations of physical performances of the blended cements reveal that the CLS glass makes little or no contribution to the early strength. The glass reactivity however increases over time and it makes considerable contribution to the late strength that is approaching that of pure Portland cement. Increase of the CLS glass surface area (to 629 m²/kg) is found to have positive effect on the strength development reaching 90% of the strength of the pure cement reference at 90 days. Combining this result with that of the CO₂ emission caused by producing blended cements containing 30 wt% CLS glass, it is concluded that the CO₂ emission can be reduced with 10% for the same performance as Portland cement. This is valid when substituting the clinker with glass on a 1:1 weight basis.

When limestone and CLS glass is added to the same cement, a synergetic effect is observed for the long term strength. This is caused by a larger fraction of the limestone participating in the cementitious reactions as the content of Al_2O_3 available for reaction with limestone is increased by introducing CLS glass to the cement. For blends containing 20% CLS glass (surface area of $629 \text{ m}^2/\text{kg}$) and 10% limestone, the 90 days strength exceeds that of Portland cement. Using these blended cements, reductions in the CO_2 release of 20% can be achieved for the same concrete performance. The use of CLS glasses as SCMs is a good approach for significantly reducing the CO_2 emission from cement production maintaining acceptable performance of the final material.

Danish abstract

Store mængder energi forbruges til fremstilling af Portland cement. Dette gør cementindustrien ansvarlig for ca. 5% af den globale menneskeskabte CO₂-udledning. Cementindustrien gør derfor et stort stykke arbejde for at sænke sine emissioner.

Strategien, der anvendes i dette studie, er at sænke CO₂-udledningen vha. klinkersubstitution. Det betyder, at klinkerne delvist erstattes af supplerende cementagtige materialer (SCMs), og dette studie omhandler udvikling af nyskabende SCMs baseret på calcium aluminosilikat (CAS) glaspartikler produceret specifikt til denne anvendelse. Formålet falder i to dele. 1) Optimering af sammesætningen af CAS glasset med henblik på at reducere CO₂-udledningen forbundet med produktion af glasset samt at sikre høj pozzulanitet. Pozzulanitet refererer til glassets evne til at tage del i dannelsen af strykegivende hydratiseringsprodukter, når glasset blandes med cement; 2) Undersøgelse af de fysiske egenskaber af blandingscementer indeholdende 30wt% af de nyudviklede SCMs samt undersøgelse af hydratiseringsprocessen for disse cements. Udover blandingscementer indeholdende én SCM undersøges også cements indeholdende både fint formalet kalksten og CAS glaspartikler.

Ud fra undersøgelser af glassets karakteristika kan det konkluderes, at et ton CAS glas baseret på de naturlige råmaterialer, ler, kalksten og sand, kan fremstilles under udledning af blot 60% af den mængde CO₂, der udledes til fremstilling af et ton klinker. Glasser baseret på disse naturlige råmaterialer referes til som CLS glas. Ydermere har glasset pozzolanegenskaber og er i stand til ved reaktion med vand og Ca(OH)₂ at danne hydratiseringsprodukter svarende til C-S-H og calcium aluminat hydratfaserne, som dannes ved hydratisering af Portland cement.

Studier af sammenhænge mellem komposition og struktur for en række glas i tre-komponent CAS modelsystemet udviser evidens for eksistensen af strukturel heterogenitet i ordenen i "mellem-udstrækning" (intermediate-range order). Dette kommer til udtryk som klyngedannelse af områder med høj grad af depolymerisation og kun begrænset indhold af Al samt områder med høj grad af polymerisation og vekslende tilstedeværelse af SiO₄ og AlO₄ tetraeder

Undersøgelse af de fysiske egenskaber for blandingscementerne viser at CLS glasset bidrager svagt eller slet ikke til den tidlige styrkeudvikling. Reaktiviteten af glasset øges dog over tid, og dette bidrager signifikant til den sene styrkeudvikling, som for blandingscementerne nærmer sig den for den rene Portland cement. Forøgelse af glaspartiklernes overflade har betydelig positiv effekt på styrkeudviklingen, som når 90% af styrken af den rene cement efter 90 dages hydratisering ved et overfladeareal på 629 m²/kg. Hvis dette resultat kombineres med CO₂-udledningen forbundet med fremstilling af blandingscementer indeholdende 30 wt% CLS glas,

kan det konkluderes, at CO₂-udledningen kan reduceres med 10% for sammen fysiske ydeevne som Portland cement. Dette er gældende for 1:1vægtbaseret substituering af klinker med glas.

For cementerne indeholdende både kalksten og CLS glas opnås en synergieffekt for den sene styrke. Det konkluderes, at baggrunden for denne er, at en større procentdel af kalkstenen tager del i de styrkegivende kemiske reaktioner, når indholdet af Al₂O₃ tilgængelig for kalkstenen til denne reaktion øges ved tilsætning af CLS glas. For blandinger indeholdende 20% CLS glass og 10% kalksten opnås 90 døgns styrker, som overstiger styrken af den rene cement. Ved anvendelse af disse cementer, kan der opnås reduktioner i CO₂-udledningen på 20% for samme 90 døgns mørtelstyrke. Alt i alt kan det konkluderes, at anvendelsen af CLS glaspartikler som SCM tilvejebringer en god mulighed for at opnår signifikante reduktioner i CO₂-udledningen forbundet med cementproduktionen, samtidig med at egenskaberne for det endelige produkt bibeholdes.

Preface

This dissertation is submitted to the Faculties of Engineering and Science, Aalborg University in partial fulfillment of the requirement for obtaining the Ph.D. degree.

The Ph.D. study is carried out at the Section of Chemistry in the Department of Biotechnology, Chemistry and Environmental Engineering at Aalborg University from August 2007 to September 2010. The study is part of the FUTURECEM project financed by the Danish National Advanced Technology Foundation. The FUTURECEM project is an interdisciplinary collaboration between Aalborg Portland A/S, GEUS (Geological Survey of Denmark and Greenland) and iNANO at University of Aarhus and Aalborg University.

Throughout the thesis the common cement chemistry abbreviations for the oxides are used when suitable. The most widely used are: C = CaO, S = SiO₂, A = Al₂O₃, F = Fe₂O₃, H = H₂O, S' = SO₃ etc. If nothing else is stated, % always refers to wt%.

I would like to thank my supervisor Yuanzheng Yue for his help, guidance and encouragement throughout this project and for the many fruitful discussions. I really enjoyed our collaboration. Kind acknowledgements also go to my collaboration partners at Aalborg Portland A/S – Duncan Herfort, Lise Frank Kirkegaard and Mette Steenberg – for all your practical assistance with performance of cement related experiments and for the many discussions regarding the challenging cement chemistry. Jørgen Skibsted and Søren Lundsted Poulsen, Instrument Centre for Solid-State NMR spectroscopy and Interdisciplinary Nanoscience Centre, Department of Chemistry, University of Aarhus deserve a special credit for performing the NMR spectroscopy investigations, and acknowledgement goes to Jens Rafaelsen, Department of Physics and Nanotechnology, Aalborg University for conducting the SEM-EDS analyses for me. I would also like to thank Joachim Deubener and Hansjörg Bornhöft, Institute for Nonmetallic Materials, Clausthal University of Technology, Germany for giving me access to use their micro penetration viscometer. Rockwool International is acknowledged for production of the CLS_{9N} glass fibers and Dantonit A/S for providing the clay for glass production. Furthermore I would like to thank all members of the FUTURECEM group for suggestions, ideas and usable outcome of our many workshops.

I would also like to express my gratitude to my colleges in the glass group. Ralf Keding deserves special mentioning for all his help in the lab and for the many useful discussions as does Lisbeth Wybrandt for always helping me out and cheering me up whether it was the experimental work or other issues bothering me. Last but not least my fellow Ph.D. colleagues deserve special recognition. Thank you for creating a good working and social environment making my last three years at Aalborg University enjoyable.

Table of Contents

1	Introduction.....	3
1.1	Background and challenges	3
1.2	Objectives of the present study.....	6
1.3	Content of the thesis	6
2	Blended cements.....	8
2.1	Portland cement.....	8
2.2	Supplementary cementitious materials	11
3	Calcium aluminosilicates in cement	13
3.1	Glasses based on pure chemicals	13
3.2	Glasses based on natural minerals	18
3.3	Summary	21
4	Blended cements containing glasses	22
4.1	Physical performances.....	22
4.2	Hydration behavior	29
4.3	Summary	35
5	Synergetic effect between limestone and glass in blended cements.....	36
5.1	Limestone as a supplementary cementitious material	36
5.2	Physical performances.....	36
5.3	Hydration behavior	39
5.4	Summary	45
6	CO₂ reduction using blended cements	46
6.1	CO ₂ release from fuels.....	46
6.2	CO ₂ release from raw materials.....	48
6.3	CO ₂ release relative to cement performance.....	49
7	General discussion and perspectives	50
8	Conclusions.....	54
9	List of references	58
A	CaF₂-CaO-Al₂O₃-SiO₂ system.....	64
B	Additional SEM-EDS results	70
	List of publications.....	74

3 Calcium aluminosilicates in cement

The approach taken in this work is to develop and engineer a glass system with the specific aim of being used as a SCM. For that purpose the calcium aluminosilicate (CAS) glass system is selected. CAS glasses can be produced in large quantities from low cost and locally available raw materials and are in addition composed of the same oxides that also constitute OPC. Thus, depolymerization of the glass in the highly alkaline environment of the cement pore solution results in Si- and Al-oxyhydroxides similar to the species that constitute the hydration phases of OPC. Glasses of this type are thus expected to participate in the formation of strength giving hydration products hence contributing positively to the performance of the blended cement mortar and concrete.

For full scale production to be economically viable the glasses should be prepared from low cost raw materials available locally in large quantities. Hence it is chosen to base the glasses on the conventional raw materials used for cement production, i.e., clay, limestone and sand, however mixed in other proportions than within cement.

It is important if a CAS glass should provide a good SCM that the production of the glass causes reduced CO₂ emission compared to the production of OPC. Equally as important is it that the glass will participate in the hydration reactions and thereby contributing to the strength of the final concrete. Thus, to determine the optimal composition of a glass system several characteristics must be balanced. In practice this is done investigating the consumption of limestone, practical melting temperature, pozzolanicity of the glass, etc.

3.1 Glasses based on pure chemicals

To simplify the understanding of the system, investigations are at first performed on a three component model system, i.e., the CaO-Al₂O₃-SiO₂ system. These are the major oxides in the natural raw materials and account for 90% of the oxides in OPC.

3.1.1 Glass characteristics

In Paper I the compositional dependence of fragility and glass forming ability (GFA) of ten CAS glasses is investigated. The glasses are divided into two series of systematic compositional changes (the eutectic series and the non-eutectic series, Figure 3.1) and are located in the vicinity of the eutectic compositions of anorthite-wollastonite-tridymite and anorthite-wollastonite-gehlenite. The glass forming ability refers to the ability of a melt to vitrify upon cooling. The critical cooling rate, i.e., the minimum cooling rate required to avoid crystallization during cooling of a melt, can be considered as a direct measure of GFA (Varshneya 1994, Shelby 2005, Ossi 2003). It is however often difficult to determine the critical cooling rate and it is of interest to use alternative methods of quantifying GFA. In Paper I it is found that

fragility, i.e., the extent of deviation from Arrhenian behavior of the viscosity-temperature relation, can be used as a measure of GFA for the CAS glasses. This is a useful evaluation method, as the fragility can rather easily be obtained from viscosity measurements.

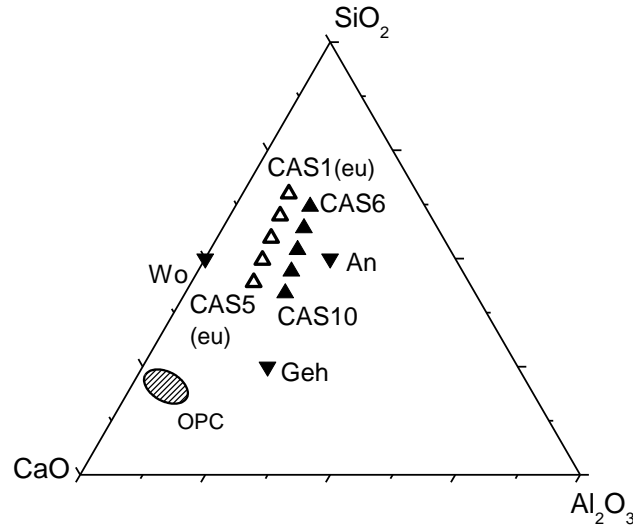


Figure 3.1: Ternary CaO-Al₂O₃-SiO₂ phase diagram (mol%). Upward triangles mark the glass compositions under investigation in Paper I. The open triangles represent the eutectic series, i.e. CAS1 to CAS5, with the end members being the eutectic composition of anorthite-wollastonite-tridymite and anorthite-wollastonite-gehlenite. The solid upward triangles represent the non-eutectic series, i.e. CAS6 to CAS10. The hatched area shows the compositional range of ordinary Portland cement (OPC) and the solid downward triangles state the composition of the geological phases wollastonite (Wo), anorthite (An) and gehlenite (Geh).

Melts with high GFA can be vitrified without forced cooling thus relating the glass forming ability to the fuel-derived CO₂ emission. Paper I concludes that the glasses in the eutectic-series in general exhibit higher GFA and that the GFA increases with increasing network polymerization. As the glasses in the eutectic series show superior GFA, the work is continued focusing on this series.

The major contributions to the CO₂ release during glass manufacture is the raw materials CO₂ release linked to calcination of limestone and the fuel-derived CO₂ release linked to the burning of fuel to reach the temperatures of production. This situation is similar to the cement production. Commonly used soda-lime-silica glasses for windows and containers are produced in the temperature range 1500-1600°C (Edgar et al. 2008).

The raw materials CO₂ release is directly related to the consumption of limestone, which is the primary source of CaO. This is valid regarding production of OPC as

well as the CAS glasses investigated in this work. Based on the composition of OPC stated in Table 2.2, the production of one ton of cement results in 516 kg of raw materials derived CO₂. In contrast, 180 kg and 300 kg CO₂ are released from the raw materials needed to produce one ton of CAS1 and CAS5, respectively. In addition to the GFA, the temperature required for melting, i.e., the practical melting temperature, affects the fuel-derived CO₂ emission for glass production. In this work, the practical melting temperature (T_{pm}) is defined as the isokom temperature corresponding to a viscosity of 10 Pa s. It is found that, $T_{pm}(CAS1) = 1527^{\circ}C$ and $T_{pm}(CAS5) = 1306^{\circ}C$ (Paper II) (Notice a different naming of the two glasses in this paper). Thus the increased content of modifying Ca²⁺ ions in CAS5 has a significant impact on the melting temperature. The determination of the practical melting temperature is described in greater detail in Paper II.

To summarize the investigations on the model system, it is found that the eutectic composition of anorthite-wollastonite-tridymite (CAS1) causes a considerable lower raw materials CO₂ emission than the eutectic composition of anorthite-wollastonite-gehlenite (CAS5), whereas the lower practical melting temperature favors the use of CAS5 compared to CAS1. Full scale production utilizing natural raw material sources will introduce a significant content of impurities e.g. alkali oxide. The presence of these impurities is expected to lead to a pronounced reduction in production temperature. Thus the reduced CaO content and superior GFA of CAS1 are considered the most important factors. This composition is chosen as the starting point for the investigations on the impure glass system.

3.1.2 Glass structure

The physical and chemical properties of glasses are determined largely by their microstructure in both short- and intermediate-range. To get a deeper understanding of the compositional dependence of the glass characteristics as described above, the composition-structure relationship of the peralkaline CAS glasses (Figure 3.1) is investigated in greater detail in Paper III. (Notice a different naming of the glasses in this paper). Especially, the clarification of intermediate-range ordering (IRO) in silicate glasses, i.e., the order extending beyond the nearest neighbors, has been of interest in recent years (Greaves, Sen 2007, Price 1996, Mauro et al. 2009a). This is also the focus point of Paper III in which the nature of the IRO is investigated by comparing the results of two different structural modeling approaches to solid-state ²⁹Si magic angle spinning (MAS) nuclear magnetic resonance (NMR) spectroscopy data. ²⁹Si MAS NMR is widely used for structural studies of aluminosilicates as the isotropic chemical shift ($\delta(^{29}Si)$) depends on both the degree of polymerization of SiO₄ tetrahedra and the presence of Al in the second coordination sphere to Si. However, simultaneously changes in the content of both network forming Al ions and network modifying Ca ions may complicate the interpretation of single-pulse ²⁹Si MAS NMR experiments. In this work, structural modeling based on the chemical composition of the glasses allows extraction of new important information about the IRO from this type of experiments. The modeling is briefly described below with a more detailed description in Paper III.

Both structural models assume similar short-range order with Si and Al acting as network formers in the peralkaline glasses. The excess Ca ions, which are not involved in the charge balance of AlO_2 units, serve to charge balance the NBOs. Based on previous investigations on peralkaline glasses a preference of Al for fully polymerized Q^4 sites is assumed in this work (Mysen 1990, Mysen, Richet 2005, Allwardt, Lee & Stebbins 2003, Lee, Stebbins 2006). The distribution of $\text{Si}(Q^n)$ units is then calculated by combinatorics assuming a statistical distribution. The next step is to describe the distribution of Al in the second coordination sphere of SiO_4 units, i.e., to describe the IRO.

The first modeling approach (R-IRO model) assumes that the structure beyond the nearest neighbors is of a random nature. The mole fractions of the 15 possible $\text{Si}(Q^{ni}(m_i\text{Al}))$ units are thus calculated using combinatorics. This results in the prediction of 7-14 non-negligible units present within each glass (Table 3, Paper III). The number of non-negligible units increases within each glass series as a function of increasing contents of NBO and Al.

In the second modeling approach (QH-IRO model), we assume a heterogeneous IRO based on the modified random network theory by Greaves (Greaves 1985). This theory predicts clustering of NBOs within silicate glasses. For the CAS glasses, clustering of NBOs is believed to result in highly depolymerized regions containing only a minor content of Al and highly polymerized regions of alternating SiO_4 and AlO_4 tetrahedra. The second modeling approach thus predicts chemical fluctuations in the IRO. The QH-IRO model predicts the presence of 4-6 different structural $\text{Si}(Q^{ni}(m_i\text{Al}))$ units for each glass (Table 4, Paper III).

To test the validity of the two IRO models, the ^{29}Si MAS NMR spectra are deconvoluted using a sum of Gaussian shaped resonances corresponding to the different types of $\text{Si}(Q^{ni}(m_i\text{Al}))$ units with relative intensities equal to the molar fractions predicted by the models.

$$f(x) = \sum_{i=1}^{15} \frac{a_i}{w \cdot \sqrt{\pi/2}} \exp \left[\frac{-2(x-x_{0i})^2}{w^2} \right] = \sum_{i=1}^{15} \frac{a_i}{w \cdot \sqrt{\pi/2}} \exp \left[\frac{-2 \left(x - \delta(Q^{ni}(m_i\text{Al})) \right)^2}{w^2} \right] \quad (3.1)$$

Thus, the ^{29}Si NMR resonances are described as a sum of Gaussian distributions (Eq. 3.1) where a_i is the relative area for a given structural unit, i.e., the molar fraction known from the modeling, x_{0i} is the center of the resonance corresponding to the chemical shift $\delta(Q^{ni}(m_i\text{Al}))$ and w is the line width. The dependencies of chemical shift on the degree of polymerization of SiO_4 tetrahedra (n : the number of BO linked to Si) and on the incorporation of Al in the second coordination sphere (m : the number of Al) are assumed to be additive and the chemical shift for a $Q^{ni}(m_i\text{Al})$ unit can be expressed by:

$$x_{0i} = \delta \left(Q^{ni}(m_i\text{Al}) \right) = \delta(Q^4(0\text{Al})) + (4 - n_i)A + m_iB . \quad (3.2)$$

Reasonable starting values of the four unknown parameters are used for the deconvolution and all ten resonances are deconvoluted simultaneously.

The intensity distribution predicted from the random IRO model cannot be validated from deconvolution of the ^{29}Si NMR resonances (Figure 3, Paper III). In contrast, the results of the heterogeneous IRO model provide convincing agreement between the deconvoluted and the experimental results (Figure 5, Paper III). This is a clear evidence of the existence of structural heterogeneity in the IRO. Paper III includes further discussions of these findings.

The structural heterogeneity in the IRO explains the only vague compositional dependence of melt fragility for the ten glasses despite increasing disorder in the short-range (Paper I). The increasing short-range disorder is caused by an increase in the content of both NBO and Al within each series. It is believed that the increasing ordering within the intermediate-range counterbalances the increasing disorder in the short-range thus resulting in only minor changes in fragility. Regarding the crystallization behavior of the glasses, the chemical fluctuations might constitute inhomogeneities capable of inducing heterogeneous nucleation or acting as nuclei for the crystallization process. This explains the superior stability of the glasses with lowest Al content (Paper III). Furthermore it is speculated, that the structural heterogeneity might show impact on the ability of the glasses to participate in the hydration processes of the blended cements. Structural heterogeneity will create weak points or defects in the structure. These will then act as starting points for the breakdown of the glassy network within the alkaline environment of the pore solution. A link might thus exist, with structural heterogeneity leading to enhanced pozzolanicity of the glasses.

3.1.3 Effect of CaF_2 on melt flow and structure

A possible method of reducing the practical melting temperature of aluminosilicate melts and thus the fuel-derived CO_2 release from production is the introduction of fluorine to the melt (Hill, Wood & Thomas 1999, Zeng, Stebbins 2000, Stamboulis, Hill & Law 2004).

Adding small amounts of CaF_2 to the CAS melts thus makes it possible to reduce the glass production temperature while at the same time slightly reducing the use of CaCO_3 to obtain a given calcium content within the glass. Appendix A describes the effect of substituting 2-8 mol% of the CaO within CAS1 with CaF_2 .

The introduction of fluorine is observed to have a pronounced effect on viscosity, reducing T_{pm} with approx. 40°C from 1527°C to 1488°C as 2 mol% CaO is substituted by CaF_2 . By ^{19}F MAS NMR the fluorine is proven to break down the network connectivity by incorporation into Al-F-Ca(n) and F-Ca(n) species with n representing the number of Ca coordinated with the fluorine. By the formation of Al-F-Ca(n) units, bridging oxygen is replaced by non-bridging fluorines, thus reducing the network connectivity.

3.2 Glasses based on natural minerals

As the eutectic composition of anorthite-wollastonite-tridymite, i.e., CAS1 (or $C_{26}A_9S_{65}$ in Paper II and III), was concluded to be the most optimal three component composition, this composition is targeted using the natural minerals as raw materials. These are all available in large quantities in Denmark, and the compositions are given in Table 2 in Paper II. The relative content of Al_2O_3 in the clay is rather close to that in CAS1. Hence, it is possible to obtain the target composition by mixing the raw materials only in the following proportions by weight: 63% clay, 31% limestone and 6% sand. This results in the composition of CLS_{1N} stated in Table 3.1. The nomenclature refers to the three raw materials and the subscript indicates the aimed molar content of Na_2O . The use of natural minerals introduces $\approx 10\%$ minor components or impurities mainly as alkali oxides, MgO and Fe_2O_3 . CLS_{5N} and CLS_{9N} , containing 5 and 9 mol% Na_2O , respectively, are produced to investigate the effect of adding additional alkali oxide. In industrial-scale production, extra alkali oxide can be introduced by recycling dust collected from the cement kiln or from albite or granite high in alkali oxide (syenite and alkali granite), or directly as Na_2SO_4 . Paper II and Paper IV are concerned with the characterization of the glasses.

Table 3.1: Oxide compositions (mol%) for the three CLS glasses. The composition of CAS1 is given for comparison. The compositions are determined by wet chemical analyses.

	CAS1	CLS_{1N}	CLS_{5N}	CLS_{9N}
SiO_2	64.9	59.1	56.1	53.9
Al_2O_3	9.3	8.2	7.9	7.7
Fe_2O_3	-	3.0	2.9	2.8
CaO	25.8	22.1	21.2	21.3
MgO	-	4.2	3.9	3.9
K_2O	-	1.7	2.0	1.6
Na_2O	-	1.2	5.4	8.2
SO_3	-	<0.1	0.2	0.2
TiO_2	-	0.5	0.5	0.5

3.2.1 Glass characteristics

The limestone content of the CLS glasses is comparable to that of CAS1, and the production of these results in ≈ 175 kg CO_2 released from limestone calcination per tonne glass produced. In addition to the raw materials CO_2 release the carbonate content also affects the fuel-derived CO_2 release as the calcination process is endothermic. From differential scanning calorimetric measurements on raw material batches of CAS1 and CLS_{9N} , the enthalpy of calcination is found to be ≈ 650 kJ/kg and ≈ 325 kJ/kg, respectively. For comparison the enthalpy of calcination of the production of PC clinker is ≈ 2100 kJ/kg (Taylor 1997).

The introduction of impurities to the glass system has a pronounced effect on the viscosity temperature relation (Figure 2, Paper II), with the viscosity being significantly reduced in the entire temperature range shifting from CAS1 to CLS_{1N} .

Upon introduction of additional alkali oxide the viscosity decreases even further. This is reflected in the values of T_{pm} (Table 3.2), that decreases with almost 200°C shifting from the pure chemical system (CAS1) to the natural raw materials (CLS_{1N}). The glasses based on natural minerals can thus be produced at temperatures in the range 1300-1350°C. This is significantly reduced compared to the production temperature of OPC.

The fragility of the melts (m) is derived from the description of the viscosity-temperature (η, T) relation using the MYEGA equation (Mauro et al. 2009b)

$$\log \eta = \log \eta_{\infty} + (12 + \log \eta_{\infty}) \frac{T_g}{T} \exp \left[\left(\frac{m}{12 - \log \eta_{\infty}} - 1 \right) \left(\frac{T_g}{T} - 1 \right) \right] \quad (3.3)$$

where η_{∞} is the infinite temperature viscosity and T_g is the glass transition temperature. The introduction of 10% minor components reduces the fragility thus increasing the glass forming ability of the melts. Similar values of m are obtained for the CLS glasses with varying Na₂O content.

Table 3.2: Characteristic temperatures and fragility indices (m) for CAS1 and the CLS glasses.

	T_{pm} (°C) ^a	T_g (°C) ^b	m (-) ^b	Degree of pozzolanic reactivity ^c
CAS1	1527	781.6 ± 0.6	49.6 ± 0.4	12
CLS _{1N}	1346	688.6 ± 1.4	43.2 ± 1.2	14
CLS _{5N}	1329	654.3 ± 0.9	44.0 ± 0.8	16
CLS _{9N}	1285	629.7 ± 0.8	43.7 ± 0.7	22

^a The practical melting temperature (T_{pm}) is given as the isokom temperature at $\eta = 10$ Pa s. The uncertainty associated with T_{pm} is estimated to be ± 3-4%.

^b T_g and m are obtained from the fit of the viscosity-temperature data using the MYEGA equation.

^c Determined as mass loss of glass during reaction with Ca(OH)₂. From repeated measurement on CLS_{9N} the uncertainty associated with the mass losses is estimated to be ± 5-10%.

To increase the ability of the glass to take part in the hydration reactions it must be crushed and ground to obtain a large surface area. As significant amounts of energy are also consumed during the crushing and grinding, the grindability of the glasses is also considered. In Paper III it is evaluated indirectly measuring the Vickers hardness (H_v) as well as the fracture tendency at a given load. Combining the results of H_v and fracture tendency, CLS_{9N} is found to have the best grindability with the lowest H_v (of the CLS glasses) and the largest fracture tendency. Thus, particle formation is expected to require the smallest energy consumption for this composition. Grinding of CLS_{1N} and CLS_{9N} in a porcelain mill confirms that particles of cement fineness are more easily obtained for CLS_{9N} than for CLS_{1N}. The duration of the grinding process of CLS_{9N} can be reduced by 6% compared to CLS_{1N}.

In addition, Figure 3.2 compares the grindability of clinker with that of CLS_{9N}. The materials are ground in a porcelain mill using steel bodies and associated values of

surface area and duration of the grinding are found. The two materials follow the same trend until a surface area of approximately 400 m²/kg. After this point the CLS_{9N} glass shows superior grindability. Particles of the fineness of the cement used in this project, i.e., 575 m²/kg, are thus more easily obtained with CLS_{9N} particles compared to the cement clinker.

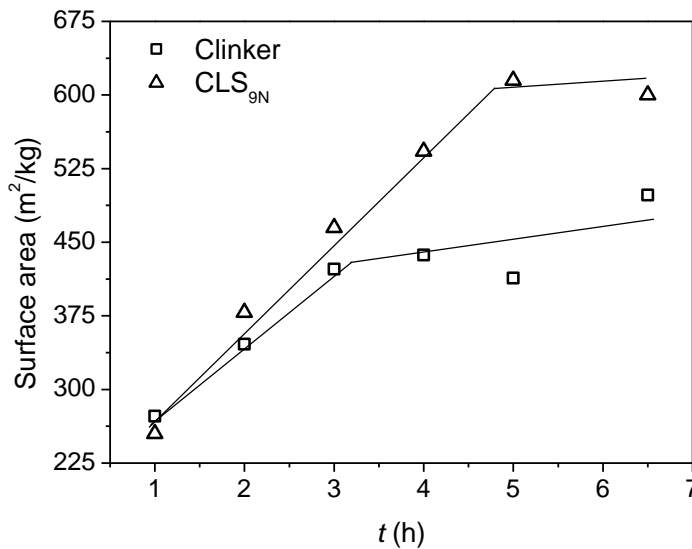


Figure 3.2: Surface area as function of grinding time for clinker and CLS_{9N} glass illustrated as the surface area vs. time of grinding in a porcelain mill. The surface area is measured by air permeability using the Blaine method. The solid lines should be regarded as guides for the eye.

3.2.2 Pozzolanity

The SCMs are often less reactive than Portland cement, and a partial substitution of OPC with SCM will thus reduce the compressive strength compared to the pure cement (Massazza 2007, Shi, Zheng 2007). To ensure acceptable performance of the final mortar or concrete without being forced to increase the content of the blended cement per cubic meter of concrete, it is of importance to minimize the reduction in compressive strength. This is possible if the SCM exhibits pozzolanity and thus contributes to the strength giving reactions taking place during hydration.

The pozzolanity of the glasses is tested as the reactivity of glass particles in a saturated Ca(OH)₂ solution. The alkalinity of the Ca(OH)₂ solution resembles the pore solution of cement paste and mortar. The degree of pozzolanity is quantified as the fraction of glass that has reacted with Ca(OH)₂ and water after 7 days at 40°C (Table 3.2). This is determined as the mass loss of glass. The pozzolanity increases as minor components are introduced to the glass system from the natural minerals and it further increases upon introduction of additional alkali oxide.

²⁷Al and ²⁹Si MAS NMR spectroscopy investigations are performed on CAS1 and CLS_{9N} to further examine the pozzolanic reactions between the calcium

aluminosilicate glasses and Ca(OH)_2 . The idea is to test if hydration phases are formed resembling the ones formed during hydration of OPC.

During OPC hydration the main hydration product is the C-S-H phase (Section 2.1.1). As this is formed the isolated SiO_4 tetrahedra (Q^0 units) of alite and belite react with water and polymerize into dimers and chains of SiO_4 tetrahedra, i.e. Q^1 and Q^2 units, that constitute the C-S-H phase (Taylor 1997, Odler 2007). During hydration the Al ions are mainly incorporated into crystalline aluminate hydration products. The hydration of the aluminate phases can be followed by the gradual conversion of tetrahedrally coordinated AlO_4 in the anhydrous cement into octahedrally coordinated AlO_6 sites present in the calcium aluminate hydrates (Taylor 1997, Odler 2007, Richardson 1999, Andersen, Jakobsen & Skibsted 2003). The ^{29}Si MAS NMR spectra of CAS1 and $\text{CLS}_{9\text{N}}$ before and after the pozzolanic test (Figure 3, Paper II) exhibit broad resonances in the range from -75 ppm to -115 ppm, reflecting the amorphous nature of the glasses including different Q^n units. Subtraction of the spectra before and after the reactivity test reveals sub-spectra which only include resonances from the hydration products. For both glasses these difference spectra show resonances in the range -75 to -90 ppm assigned to Si in Q^1 and Q^2 units. This indicates the formation of a chain-like silicate structure during the reaction with Ca(OH)_2 and water.

In ^{27}Al MAS NMR, resonances in the range 55 to 80 ppm are expected for AlO_4 units whereas AlO_6 octahedra result in resonances with chemical shifts from -15 to 20 ppm (Merzbacher et al. 1990, Muller et al. 1981). The ^{27}Al MAS NMR spectrum of CAS1 (Figure 4, Paper II) includes a broad resonance corresponding to Al in tetrahedral coordination. In addition to tetrahedrally coordinated Al the ^{27}Al MAS NMR spectrum of $\text{CLS}_{9\text{N}}$ (Figure 4, Paper II) reveals that a small fraction of the Al is present in octahedral coordination for this sample. The corresponding spectra of the glasses after the pozzolanic reactivity test reflect that a hydration product including octahedrally coordinated Al in a more ordered phase has formed.

The glasses are thus concluded to be pozzolanic active forming hydration products similar to the phases formed during hydration of OPC. These NMR investigations are described in greater detail in Paper II.

3.3 Summary

It is demonstrated that calcium aluminosilicate glasses can be produced at reasonable conditions, i.e. relatively low production temperature and without artificial cooling to avoid crystallization, employing the natural deposits of clay, limestone and sand as raw materials. Addition of extra alkali oxide or minor contents of CaF_2 further reduces the energy consumption required for production. Furthermore the calcium aluminosilicates are pozzolanic active and are thus expected to participate in the strength given reactions during hydration of blended cements containing the glasses.

4 Blended cements containing glasses

The reactivity test of aqueous glass- $\text{Ca}(\text{OH})_2$ mixtures proved that the CAS glasses are pozzolanic active. This is valid for the glasses based both on pure chemicals and on impure natural minerals (the CLS glasses), however with the latter possessing the greatest reactivity. These glasses are thus expected to contribute positively to the strength of blended cements by chemical means, i.e., the glass is expected to take part in formation of strength giving hydration phases.

The effect on physical performance of adding CAS glass to Portland cement is more directly investigated by preparing blended cement pastes and mortars analyzing these by suitable methods. In the present work, blended cements containing 30 wt% clinker replacements are prepared. Mortar specimens are used to test workability and mechanical performance and paste samples are used to further investigate the hydration behavior of the blended cements.

The investigations of glass characteristics (section 3.2.1, Paper II) showed that the introduction of additional Na_2O to $\text{CLS}_{9\text{N}}$ as compared to $\text{CLS}_{1\text{N}}$ (obtained by directly mixing the natural minerals) has a positive impact both on the energy consumption during production and on the degree of pozzolanicity. In addition $\text{CLS}_{9\text{N}}$ also showed improved grindability compared to $\text{CLS}_{1\text{N}}$. This implies $\text{CLS}_{9\text{N}}$ particles to be the best candidate as a suitable SCM. On the other hand, high contents of alkalis in the cement pore solution might cause alkali-silica reactions to occur in concretes exposed to moisture. In these reactions, hydroxide ions in the pore solution react with reactive silica from the aggregates forming a gel that can take up water. The water-taking effect causes volume changes that might lead to crack formation in the concrete (Taylor 1997, Lawrence 2007a). Hence it is of importance that the alkalis of SCMs rich in alkali oxide are incorporated into the hydration phases instead of being dissolved in the pore solution. Mortars containing both $\text{CLS}_{1\text{N}}$ and $\text{CLS}_{9\text{N}}$ are prepared.

4.1 Physical performances

The suitability of the CAS glasses as an alternative to the conventional SCMs is tested comparing the physical performance of mortars containing CAS glass particles to that of mortars containing fly ash. The effects of particle surface area as well as cooling conditions during production of the CAS glasses are also investigated. This is the topic of Paper V and VI. The experimental methods used to test the physical performance are described in these papers.

Table 4.1 lists the different SCMs tested. $\text{CLS}_{9\text{N}}$ is ground to two different surface areas and the melt of this composition is in addition spun into fibers using the cascade spinning process (Širok, Blagojević & Bullen 2008). The fibers are produced by Rockwool International A/S, Hedehusene, Denmark and are subsequently ground to the same fineness as one of the $\text{CLS}_{9\text{N}}$ samples. The effect of the fast cooling is elaborated in section 4.1.1. The fly ash is a low-CaO ash with approx. 5 wt% CaO

(composition given in Table 1, Paper V) and it is included in the investigations to represent a traditional SCM. The inert filler is coarse quartz particles. Aplite, a crystalline material consisting primarily of quartz and alkali feldspar, is also tested to elaborate the difference between crystalline and amorphous materials.

Table 4.1: Size characteristics of the SCMs under investigation.

SCM	CLS _{1N}	CLS _{9N}	CLS _{9N fine}	CLS _{9N fiber}	Fly ash	Inert filler	Aplite
Surface area (m ² /kg) ^a	338	371	629	619	330	n/a	422
D ₅₀ (μm) ^b	16.2	14.4	6.0	6.2	20.1	D _{max} < 90 μm	16.9

^a Determined by air permeability using the Blaine method

^b 50% fractile determined by laser diffraction

4.1.1 Excess energy stored in the glass

The CAS glasses are produced by cooling the glass melt fast enough to avoid crystallization. The degree of disorder in the glass depends on the cooling rate. The faster the cooling rate the higher the temperature at which the structure is frozen-in, and the higher the degree of disorder and thus the stored excess energy of the final glass. An increasing structural deviation from equilibrium will yield a less stable glass expected to demonstrate a higher degree of reactivity within the blended cement. To test this hypothesis, two glasses with different degrees of stored excess energy are produced employing different cooling rates.

High cooling rates can be achieved by drawing thin fibers from the glass melt. In this work, discontinuous fibers with diameters of 3-15 μm are produced from the CLS_{9N} melt using the cascade spinning process as mentioned above. This yields cooling rates of about 10⁶ K/s. In contrast, the normally cooled glasses, which are cast onto a graphite plate is cooled at about 10³ K/s. The cooling rates are calculated using the procedure reported in (Yue, von der Ohe & Jensen 2004).

The excess energy stored in the glass can be determined from the heat capacity curves of the first and second upscan obtained by differential scanning calorimetry (Yue, Christiansen & Jensen 2002). Normal heating and cooling rates of 10°C/min must be employed for both scans. Figure 4.1 depicts the heat capacity curves for CLS_{9N fiber}. The first upscan (C_{p1}) reflects the thermal history of the glass, e.g. the cooling rate used during preparation of the glass, whereas the second upscan (C_{p2}) reflects the thermal history of the glass cooled at 10°C/min. The difference between C_{p2} and C_{p1} equals the enthalpy release. Fast cooling during production results in a large amount of enthalpy stored in the glass. The total enthalpy release during the entire heating process is found as the integral of $C_{p2} - C_{p1}$, i.e., the area between the two curves. This equals the total excess energy (ΔE_{tot}) stored within the glass (Yue, Christiansen & Jensen 2002). As comparison, the heat capacity curves of the normally cooled CLS_{9N} glass are illustrated in Figure 4.2. It is found that, $\Delta E_{tot}(CLS_{9N}) = 7.1 \text{ J g}^{-1}$ and $\Delta E_{tot}(CLS_{9N fiber}) = 84.4 \text{ J g}^{-1}$. Thus, the increased cooling rate of fiber production has a significant impact on the excess energy stored in the glass and hence on the stability of the glass.

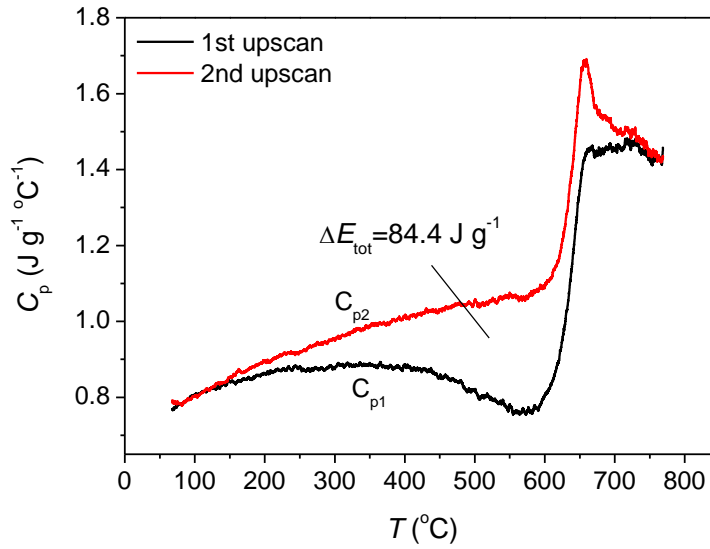


Figure 4.1: Heat capacity curves of the rapidly cooled CLS_{9N} fibers. Cooling and heating rates of 10°C/min are employed for both scans. The total excess energy stored within the glass (ΔE_{tot}) is found as the area between the two curves.

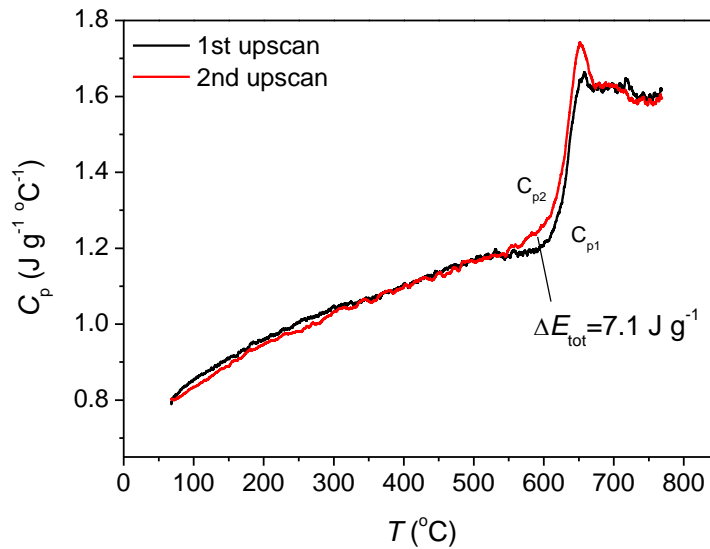


Figure 4.2: Heat capacity curves of the normally cooled CLS_{9N} glass. Cooling and heating rates of 10°C/min are employed for both scans. The total excess energy stored within the glass (ΔE_{tot}) is found as the area between the two curves.

4.1.2 Workability

The workability of concrete or mortar refers to the ease of mixing, transporting, placing and compacting it to a uniform material (Taylor 1997). In this work the workability is measured at a constant water to cement ratio. For all the SCMs tested

(Table 4.1), standard mortar workability is slightly improved with increased slump on the flow table of 2-8 % compared to the pure cement mortar. This is a major advantage compared to calcined clay based SCMs also investigated in the FUTURECEM project, as these significantly reduce the workability requiring additional water or addition of superplasticizer (He, Osbæk & Makovicky 1995, FUTURECEM Unpublished data).

4.1.3 Setting behavior

The physio-mechanical changes taking place during cement hydration is as mentioned in section 2.1 divided into setting and hardening. The setting refers to the loss of plasticity of the fresh mortar as it is converted into a solid material, and the hardening is the development of hardness and strength of the solidified mortar (Nepper-Christensen 1985, Odler 2007).

The initial part of the hydration is associated with evolution of heat. The setting behavior and the initial strength development can thus be characterized by measuring the rate of heat evolution during the first hours of hydration. The heat evolution of all the blended cement mortars follows the expected pattern (Figure 1, Paper V). Immediately after mixing of cement, sand and water, a rather fast evolution of heat is observed. This is the effect of wetting the solid materials and partial dissolution of their surfaces. Formation of small quantities of the hydration products are expected during this period. A decrease in the heat evolution due to the existence of an induction period is followed by the main exothermic peak. During this period, the actual formation of hydration phases occurs and the cement paste sets (Odler 2007). The heat of hydration of all the blended cements is lower than that of the pure cement, indicating that the clinker is replaced by a less reactive material (Figure 1, Paper V).

To make the effect of the SCM more clear the heat evolution is normalized by the Portland cement fraction in the blend. This is done in Figure 4.3. CLS_{1N} and CLS_{9N} show similar behavior and only CLS_{9N} is included in the figure. Although all SCMs are concluded to be less reactive than OPC both fly ash and aplite contributes to the early hydration. For these samples the heat evolution accelerates faster than for the reference in the beginning of the second heat release and the height of the main peak is in addition slightly increased. The reason for this is believed to be that the SCM particles act as nucleation sites for the early alite hydration. This has been reported previously with various finely ground SCMs (Hjort, Skibsted & Jakobsen 1988, Krøyer et al. 2003). On the other hand, the glass does not appear to make any contribution to the early hydration having heat development patterns resembling the inert material. The reduced intensity of the main peak compared to the pure cement mortar even suggests that the presence of 30 wt% glass retards the early hydration of the cement.

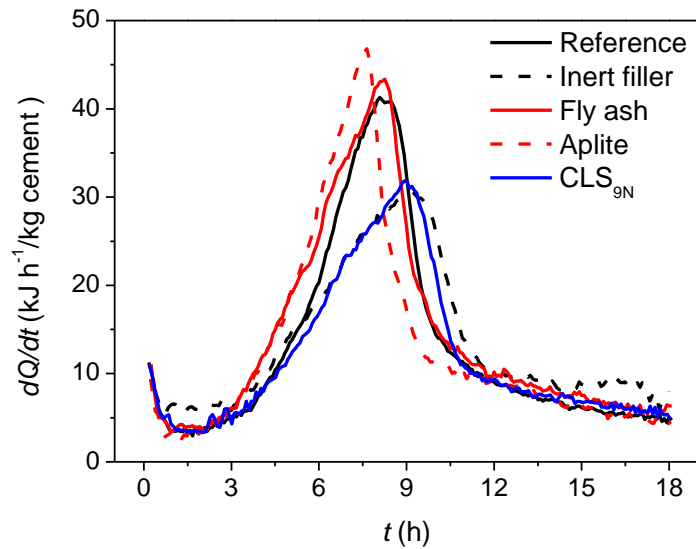


Figure 4.3: Setting behavior measured as the rate of heat evolution normalized by the fraction of Portland cement within the blended cement. The heat evolution (dQ/dt) is plotted as a function of the hydration time (t).

Figure 4.4 shows the effect on setting behavior of increasing the surface area of the glass particles and of increasing the excess energy stored in the glass. Surprisingly the increase of surface area does not show an impact on the main heat release. In contrast, the rapidly cooling significantly increases the intensity of the main peak approaching the size of the pure cement peak. Thus, increasing the structural disorder and hence the ease of bond breaking within the glassy particles increases the participation of the glass in the initial hydration.

Based on six repeated measurements on OPC paste samples, estimates of the uncertainty associated with the semi-adiabatic measurements can be deduced. From this it is found that the onset and offset temperatures of the second heat release can be given with an accuracy of approximately $\pm 10\%$, whereas the total heat release within the first 18 hours can be given an accuracy of $\pm 5\%$. This is assumed to be valid with all measurements.

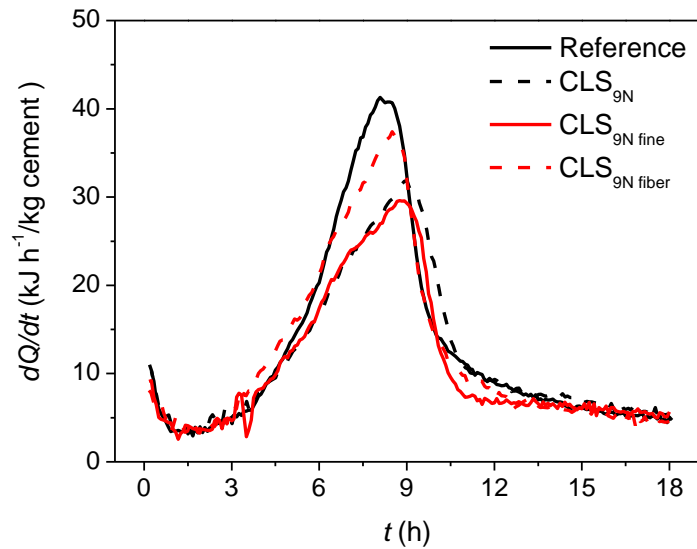


Figure 4.4: Setting behavior measured as the rate of heat evolution normalized by the fraction of Portland cement within the blended cement. The heat evolution (dQ/dt) is plotted as a function of the hydration time (t).

4.1.4 Compressive strength

The compressive strength (hereafter referred to as strength) is the most important material parameter used to characterize cement-based products. Figure 4.5 compares the strength development up to 90 days normalized by the strength of the pure cement mortar (σ/σ_{rel}) of the blended cements containing the various SCMs. CLS_{1N} and CLS_{9N} show comparable behavior (Figure 2, Paper V) and only CLS_{9N} is included in this figure. The pozzolanic reactivity of the CLS glass and fly ash is apparent, as the strength of the mortars containing these materials is significantly higher than that of the mortar containing quartz. For CLS and fly ash the relative strength reaches approximately 75% at 90 days compared to 55% for the quartz containing mortar. The pozzolanic reactions of the CAS glasses and fly ash are however limited at early stages of hydration ($\sigma/\sigma_{rel} \approx 50\%$ after 1 day of hydration) but increases over time. The superior behavior of the fly ash containing cement found during the first 18 hours hydration (Figure 4.3) is not reflected in the compressive strength measurements. Here similar strength development patterns are observed for the three SCMs (CLS_{1N} , CLS_{9N} , fly ash). The aplite containing cement exhibits a strength development pattern in between the CLS glasses and the inert filler. The early strength of the aplite cement is significantly increased as compared to the quartz containing cement. Again this is expected to be due to the aplite particles acting as seeds for the early alite hydration. A constant relative strength of 60% is reached after 28 days for the aplite containing cement compared to 55% for the inert filler. The blended cements containing fly ash and CLS glass do not reach a constant relative strength after 28 days. In contrast the strength increases steadily up to 90 days.

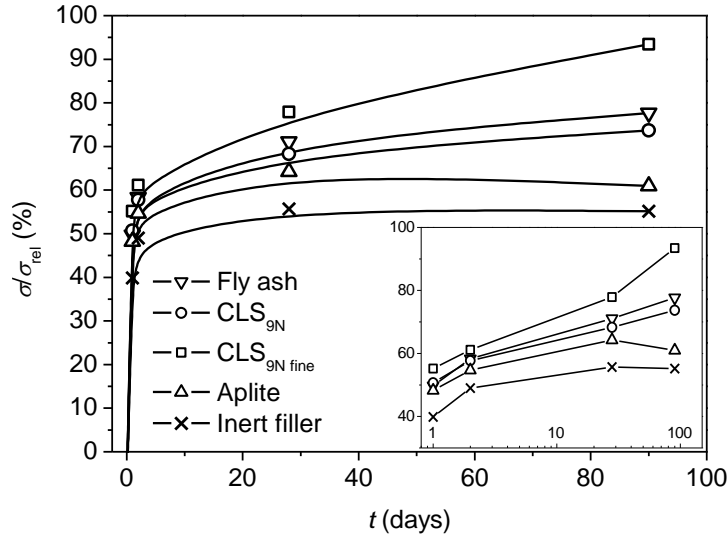


Figure 4.5: Strength development of blended cement mortars containing different SCMs. The strength is given relative to the strength of pure Portland cement mortar (σ/σ_{rel}) as a function of hydration time (t). The inset shows the strength development on a logarithmic time scale.

From repeated measurements on the reference samples, the uncertainty associated with the strength measurements is found to be in the range of $\pm 5-10\%$. This is believed to be a good indication of the uncertainty associated with all measurements. Figure 4.5 also shows the effect of grinding the glass to a higher surface area. As expected, this results in a significant acceleration of strength development reaching above 90% of the pure cement strength after 90 days of hydration. At durations longer than examined in the heat evolution measurements (i.e., 18 hours) the surface area thus seems to be a limiting factor for the reactivity of the coarse glass particles. Contrary to this, the blended cement mortar containing the fast cooled fibers only shows slightly higher 90 day strength than that of the mortar containing normally cooled glass (Figure 3, Paper V). Despite the significant impact on setting behavior of the degree of structural disorder, the effect on compressive strength is limited.

Cements are often classified in terms of the 28 days mortar strength, and three different classes are found in the European Cement Standard, i.e., 32.5, 42.5 and 52.5. The names refer to the minimum strength (in MPa) achieved after 28 days of hydrations following the measurement procedure of the European Standard EN 196-1. The compressive strength obtained within this work for the mortars containing pure OPC corresponds to 65.9 ± 0.8 MPa following the measurement procedure of EN 196-1. The strength of the mortars containing pure OPC is thus larger than the minimum requirement. This allows cements of relatively reduced strength to be used

for certain applications. The blended cements containing both the coarse and the fine CLS_{9N} glass particles fulfill the strength requirements to the class 32.5 and 42.5 cements.

4.1.5 Summary

From the investigations of workability, setting behavior and compressive strength of mortar specimens, the performance of blends containing either CLS_{1N} or CLS_{9N} cannot be distinguished. The CLS glasses are found not to contribute to the setting and initial hydration of the mortars, whereas the contribution to strength development is significant. The strength development of CLS glass containing mortars is comparable to that of mortars containing fly ash.

An increase of the structural disorder within the glass reduces the restraint of the initial setting (within the first 18 hours of hydration) otherwise observed for the glass containing blends. On the other hand an increased particle surface area significantly increases the compressive strength of the mortar. In general, the CLS glass particles can be concluded to provide a promising alternative SCM with acceptable mortar workability and compressive strength.

4.2 Hydration behavior

The hydration behavior of the CLS glass containing cement blends is investigated in greater detail using paste samples. It is of interest to determine how the introduction of 30 wt% glass of higher SiO₂ and Al₂O₃ content affects the formation of hydration phases. The glass particles with the largest surface area are chosen for this examination. The physical performances evaluated as the strength are for this sample found to be significantly improved compared to the coarse CLS_{9N} particles, implying that it reacts to a greater extent. Paper VII is concerned with the hydration behavior of these paste samples describing the experimental conditions for the paste preparation, the ²⁹Si MAS NMR and XRD investigations, and the thermal analyses.

4.2.1 Identity of hydration phases formed after 90 days of hydration

In addition to the six main components of OPC namely CaO, SiO₂, Al₂O₃, SO₃, Fe₂O₃ and H₂O, the 30% CLS_{9N} blended cement contains significant contents of alkali oxide with 2.0 wt% Na₂O_{eq} compared to 0.5 wt% Na₂O_{eq} for OPC (composition given in Table 2.2). Another SCM relatively high in alkali is fly ash normally containing up to 5 wt% Na₂O_{eq} compared to 9 wt% in CLS_{9N}. For fly ash containing cements the capacity of the C-S-H phase to incorporate alkalis is observed to increase as the content of acidic oxides, i.e. SiO₂ and Al₂O₃, increases (Chunxiang, Hongding & Xianghui 1994, Duchesne, Bérubé 1994). It is of interest to determine whether a similar incorporation takes place within the CLS_{9N} containing cement pastes.

From the ^{29}Si MAS NMR spectroscopic investigations described in Paper VII it is concluded that approximately 50% of the glass ($\text{CLS}_{9\text{N fine}}$) has reacted chemically within 90 days of hydration. In addition, Paper VII reach the conclusion that the cement is almost fully hydrated within 90 days as only traces of the clinker minerals alite and belite are found. This results in a reactive mix of composition given in Figure 4.6 (referred to as the $\text{CLS}_{9\text{N}}$ reactive mix). The position of the mix is displaced towards higher Al_2O_3 and SiO_2 contents compared to OPC. The $\text{CLS}_{9\text{N}}$ reactive mix is however still positioned within the same phase field as OPC with expected formation of CH, C-S-H, ettringite, monosulfate as well as iron oxide and pore solution (Section 2.1.1).

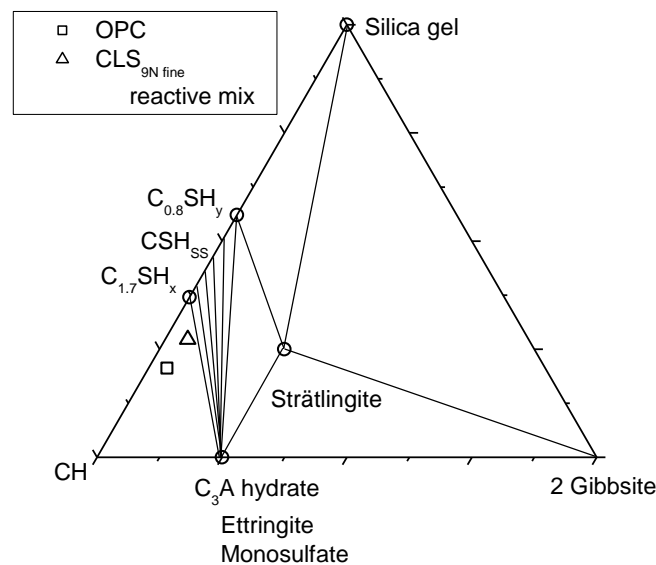


Figure 4.6: CAS (H) sub-ternary phase diagram (mol%) showing the location of the reactive $\text{CLS}_{9\text{N fine}}$ -cement mix and that of ordinary Portland cement (OPC) and the hydration phases expected to be formed. In addition, to the phases predicted by the phase diagram, iron oxide and pore solution are present in excess, i.e. plotting outside the phase diagram.

By XRD the following phases are identified in the OPC paste hydrated for 90 days: CH, C-S-H ($\text{Ca}_{1.5}\text{SiO}_3 \cdot 5\text{H}_2\text{O}$), monosulfate and ettringite. Probably due to a low content, no iron oxide is detected (Figure 1 and Table 4, Paper VII). This is in agreement with the phase assemblage predicted from Figure 4.6. In addition to the phases identified for the OPC cement, Na-C-S-H ($\text{Na}_2\text{CaSiO}_6 \cdot 2\text{H}_2\text{O}$) is identified in the $\text{CLS}_{9\text{N}}$ reactive mix. As a C-S-H phase of such low C/S ratio, i.e., $\text{C/S} = 1$, is not expected to co-exist with free CH (Figure 4.6), this is believed to be an artefact formed from precipitation from the pore solution during sample preparation. In OPC the majority of the alkalis are dissolved in the pore solution however with minor contents bound into the solid hydration phases mainly the C-S-H phase. The capacity of the C-S-H phase to incorporate alkalis increases as the content of acidic oxides,

i.e. SiO_2 and Al_2O_3 , increases. Its capacity to bind alkali is thus very limited at $C/S = 1.75$ as expected for OPC. It however increases significantly for C/S ratios below 1.5 (Chunxiang, Hongding & Xianghui 1994, Duchesne, Bérubé 1994, Hong, Glasser 1999). The ability of the C-S-H phase formed within the CLS_{9N} blended cement to take up alkalis is thus expected to be limited. Hence, it requires additional experiments, e.g. test of alkali content in pore solution or expansion of mortar bars, to draw any final conclusions on the risk of expansion due to alkali-silica reactions.

Identification of hydration phases by SEM-EDS

The hydrated phases are additionally examined by scanning electron microscopy – energy dispersive spectroscopy (SEM-EDS) using a Zeiss 1540 XB focused ion beam, EDS, EBDS at Nanolab, Aalborg University, Denmark. For the SEM examinations of cement pastes a backscatter detector is used to maximize the contrast from compositional differences. In such images the brightest areas correspond to the unreacted clinker phases, CH is observed as darker areas than the unreacted clinker but brighter than the other hydration products, whereas the pores will appear black (Taylor 1997). For SEM-EDS analyses the pastes are after 90 days of hydration cast in epoxy, ground, polished and stored in a dessicator until the measurements are performed. Using EDS the chemical composition of individual spots can be determined. To make such investigations, it is important to examine areas large enough to represent the entire sample but at the same time of a sufficiently high magnification to distinguish the different phases. In this work, a magnification of 1800 is used and EDS data are collected from three images from various locations within the sample. The measurement depth is dependent on the acceleration voltage used during the measurement. High voltages result in large measurement depths. To obtain good separation of the phases a low acceleration voltage and thus energy must be employed during the measurement. It is however also of importance to use a sufficiently high energy to excite all relevant components. In this work, the EDS measurements are performed at 15keV. This gives a measurement depth of approximately $1.5 \mu\text{m}$. The EDS data are collected performing a spectral imaging of the entire sample including all elements. The entire image is scanned for one element, before scanning for the next. This might introduce a small drifting of the image resulting in a reduced separation of the phases. A total of ≈ 1200 spots (400 from each image) are analyzed for each sample. The data interpretation are made plotting the atomic percentages of the elements of interest relative to the atomic percentage of Ca, e.g. as Al/Ca vs. Si/Ca (atom%). The combination of relatively large excitation energy (15keV) as well as some drifting of the image during data collection resulted in a poor separation of the various phases. Several trends can however still be found from the SEM-EDS analyses.

Figure 4.7 shows a plot of Al/Ca ratios against Si/Ca ratios of the OPC sample. Most of the analyzed data points cluster around the line representing mixtures of CH and C-S-H but also reveals the presence of C_3A hydrate containing spots. A similar plot for the $\text{CLS}_{9N \text{ fine}}$ containing cement paste is shown in Figure 4.8. A significant

amount of the spot analyses again cluster around the line representing CH and C-S-H mixtures. In addition, a tendency of a higher fraction of spots high in SiO_2 and Al_2O_3 although still with compositions close to the C-S-H phase is found. This suggests the possibility that additional SiO_2 and Al_2O_3 are incorporated in the C-S-H phase. Furthermore a significantly larger fraction of spots clustering around the line towards C_3A is observed for this sample compared to OPC. This is in agreement with the changed composition of the $\text{CLS}_{9\text{N}}$ reactive mix. In this sample spots of rather high Al/Ca and Si/Ca ratios are present. These fall around a line from the composition of C-S-H towards that of the unreacted $\text{CLS}_{9\text{N}}$ glass, indicating significant amounts of unreacted glass left. Plots of S/Ca ratios vs. Al/Ca ratios indicate that the C_3A hydrate is primarily monosulfate (Appendix B, Figures B.1 and B.2). This corresponds to previous results on OPC pastes (Taylor 1997, Odler 2007, Nielsen, Herfort & Geiker 2005). There is however a clear indication that the $\text{CLS}_{9\text{N}}$ containing cement has higher monosulfate content than the pure OPC. As additional SO_3 is not introduced, this is in agreement with the higher fraction of points clustering around the line towards C_3A hydrates for the glass containing sample.

Thus in general the conclusions drawn from the SEM-EDS analyses agree with the phases identified by XRD. Figure 4.9 illustrates one of the three SEM images on which the results of Figure 4.8 are based. The angular and rather bright areas, four of which are marked by circles, are the unreacted glass embedded in a matrix of hydration phases.

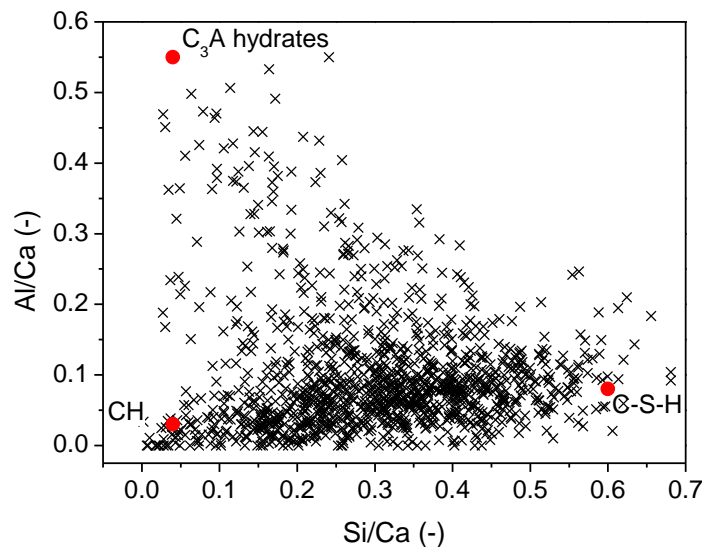


Figure 4.7: Al/Ca ratios as a function of Si/Ca atomic ratios for EDS spot analyses based on spectral imaging of an OPC paste hydrated 90 days. The atomic ratios of the hydration phases are adapted from (Odler 2007).

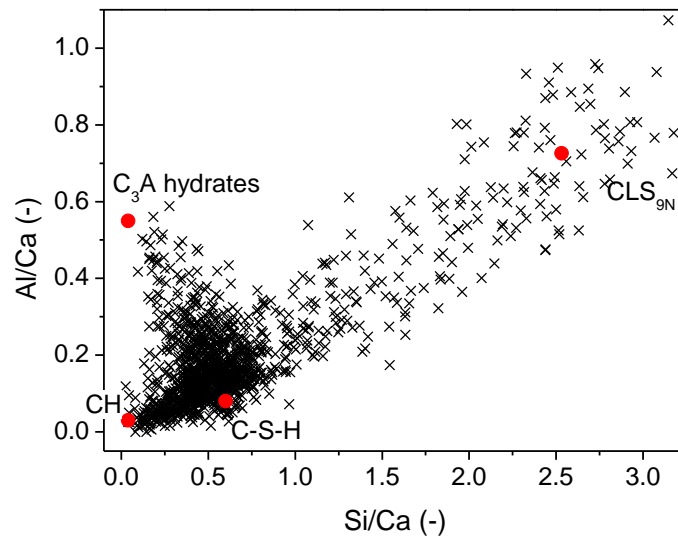


Figure 4.8: Al/Ca ratios as a function of Si/Ca atomic ratios for EDS spot analyses based on spectral imaging on a blended cement paste containing 30 wt% CLS_{9N} fine and hydrated 90 days. The atomic ratios of the hydration phases of OPC are adapted from (Odler 2007). CLS_{9N} marked on the plot corresponds to the composition of anhydrous glass.

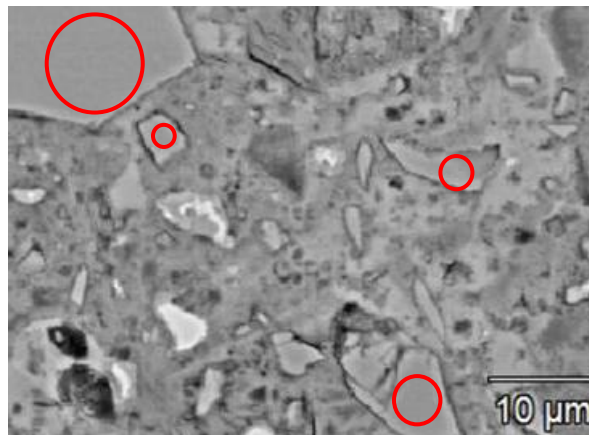


Figure 4.9: Backscattered SEM image of the CLS_{9N} fine blended cement paste hydrated for 90 days. The angular and rather bright areas, four of which are marked by circles, are the unreacted glass embedded in a matrix of hydration phases.

4.2.2 Portlandite content

The Portlandite content within the cement pastes hydrated 90 days is determined in Paper VII by means of thermal analyses from the mass loss in the temperature range 440-540°C (Figure 3, Paper VII). The CLS_{9N} cement paste is found to have a significantly lower CH content (12 wt%) than the pure cement (19 wt%). This is due to the dilution of clinker in the blended cement but also due to the CH consumption

during the pozzolanic reaction to form C-S-H with a higher Ca/Si ratio than that of CLS_{9N}.

SEM-EDS analyses of the blended cement paste containing CLS_{9N fine} after 28 days of reaction (Figures B.3, B.4 and B.5 in Appendix B) suggest a larger content of CH present, at this earlier state of hydration. As the pozzolanic reaction is most pronounced at the later stage of hydration, this can explain the larger amount of CH containing spots after 28 days of hydration compared to 90 days.

4.2.3 Reactivity of anhydrous clinker minerals and glass

The reaction of alite, belite and glass as a function of hydration time is in Paper VII determined by deconvolution of ²⁹Si MAS NMR resonances corresponding to different durations of hydration. Figure 4 in Paper VII shows the degree of hydration of alite and belite against time whereas Figure 5 in Paper VII illustrates that of CLS_{9N}. As expected alite reacts fast during the first days of hydration. The blended cement shows an accelerated alite hydration compared to the pure cement. As mentioned, this is previously reported for cements containing finely ground SCMs (Hjort, Skibsted & Jakobsen 1988, Krøyer et al. 2003) but could not be observed for the glass measuring the heat evolution during the first 18 hours of hydration (section 4.1.3). After 90 days hydration comparable degrees of alite reactivity (above 90%) are however observed for the reference and the blended cement. Significant belite reactivity is not observed until after 4 days of hydration, with the final reactivity of the blended cement being 65%. In contrast, the belite reactivity reaches 75% for the OPC paste. This is in agreement with the slightly reduced 90 days strength observed for the CLS_{9N fine} cement compared to the pure cement.

As expected the glass makes little or no contribution to early hydration, and significant glass reactivity is not observed until about 7 days of hydration. After 90 days, the degree of glass hydration is approximately 50%. As explained in Paper VII this determination is however associated with larger uncertainty than the alite and belite quantifications.

A recent ²⁹Si NMR study of blended cements containing OPC and 30 wt% natural pozzolan or fly ash used the same procedure as used in this work to determine the reactivity of the SCMs (Poulsen, Jakobsen & Skibsted 2009). Both SCMs have surface areas comparable to the fine CLS glass particles used in this work. In the study by (Poulsen, Jakobsen & Skibsted 2009), fly ash was found to have a reactivity of approximately 20% after 90 days hydration, whereas a slightly larger reactivity of approximately 25% is reported for the natural pozzolan. Despite the uncertainties associated with the glass quantification, the CLS_{9N} reactivity can be concluded to be larger than that of both fly ash and natural pozzolan. This increased reactivity of the glass compared to fly ash is however not reflected in the strength measurements in this work. In this work, similar 90 day strengths are observed for the cements containing CLS_{9N} glass particles and fly ash (Section 4.1.4). It should however be noticed that these strength measurements are made using SCM of significantly lower surface area than the SCMs used in the pastes investigated with ²⁹Si NMR.

4.3 Summary

The examination of physical performance of the various blended cements suggests the CLS glass particles to be a suitable alternative to the traditional SCMs. Particle surface area has great impact on the strength development whereas the different alkali contents of the two CLS glasses do not show any difference regarding mortar workability, setting behavior or compressive strength. Adding 30% CLS_{9N} with a surface area of 629 m²/kg gives a 90 days strength of 90% compared to OPC.

Significant glass reactivity is observed after 7 days of hydration with approximately 50% of the glass reacting in 90 days. This is expected to increase for longer durations of hydration. Similar hydration phases as formed for OPC are identified for the CLS_{9N} containing cement.

5 Synergetic effect between limestone and glass in blended cements

In addition to blended cements containing one SCM, the effect of combining two SCMs in the same cement is examined in this chapter. For these investigations blended cement mortars are prepared containing combinations of the pozzolans stated in Table 4.1 and limestone (surface area 1288 m²/kg). Thus limestone and one additional SCM are added. A clinker replacement level of 30 wt% is again used for all samples, whereas different ratios between the pozzolan and limestone are employed. Investigations are performed both regarding the physical performance of mortars and as a more detailed study of the hydration behavior of pastes.

5.1 Limestone as a supplementary cementitious material

By volume limestone is today probably the most commonly used clinker replacement material (Taylor 1997, Vuk et al. 2001, Tsivilis et al. 2003, Tsivilis et al. 1999, Zelic et al. 1999, Ramachandran 1988). The softness of limestone causes its considerable fineness when interground with cement. This accounts for the improved physical properties of Portland limestone cement (Taylor 1997, Vuk et al. 2001, Tsivilis et al. 1999). In addition, limestone is observed to participate in the hydration reactions reacting chemically with available alumina to form the so-called CO₂-AFm phase often referred to as the monocarbonate phase. The quantity of limestone reacting is however limited and reported to be in the range from a few percent to about 10% depending among other things on the C₃A content of the cement (Taylor 1997, Zelic et al. 1999, Ramachandran 1988, Klemm, Adams 1990).

The reaction sequence of C₃A for Portland limestone cement is reported to be similar to that of OPC. The fast C₃A hydration kinetics and the high gypsum solubility ensure rapid ettringite formation. As the sulfate is depleted and C₃A continues to react, the ettringite is continuously converted into the monosulfoaluminate phase (monosulfate). The calcium carbonate dissolves slowly and then reacts with any monosulfate to form an AFm carboaluminate (monocarbonate) phase. This is a more stable phase than the monosulfate due to its lower solubility. At low carbonate contents, hemiacarbonate is in addition observed (Ramachandran 1988, Klemm, Adams 1990, Péra, Husson & Guilhot 1999, Ramachandran, Chun-mei 1986).

5.2 Physical performances

As for the blended cements containing just one SCM the physical performance of the mortars containing both limestone and a pozzolan is tested in terms of the workability, setting behavior and mechanical performance. For each of the SCMs in Table 4.1 four mortar samples with varying ratios between the pozzolan (*P*) (including the inert filler) and limestone (*L*) are prepared. *P*/(*P*+*L*) ratios of 0, 0.33,

0.67 and 1 are used. Paper V and VI deal with these investigations describing the experimental conditions.

5.2.1 Workability

Limestone addition does not affect the measured mortar slump on the flow table, and the workability of mortars containing two SCMs is similar to that of the mortars containing just one. The workability is thus slightly improved compared to OPC and neither additional water nor superplasticizers are required to obtain an acceptable mortar flow.

5.2.2 Setting behavior

The setting behavior of the limestone containing mortar blends relative to the content of cement is seen in Figure 5.1. This type of plot reveals an accelerated early hydration with the intensity of the main peak being larger for the Portland limestone cement than for the pure cement. This behavior is reported previously, with the small limestone particles expected to act as seeds for the initial C-S-H formation (Klemm, Adams 1990, Péra, Husson & Guilhot 1999, Ramachandran, Chun-mei 1986). A similar behavior is observed for the mortars containing fly ash and aplite (section 4.1.3). The mortars containing two SCMs exhibit a setting behavior in between that of the two boundary blends, i.e., the mortars containing only one of the SCMs. This is illustrated in Figure 5.1 using CLS_{9N fine} as an example. A similar plot not accounting for the different cement fractions within the samples is seen in Figure 4 in Paper V.

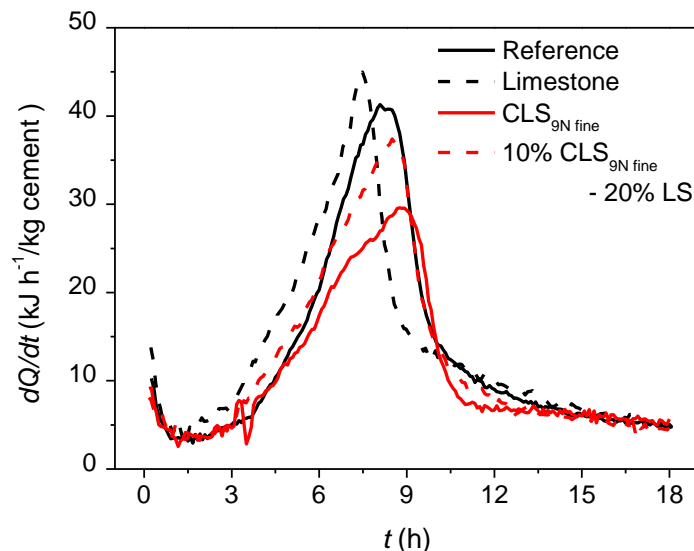


Figure 5.1: Setting behavior measured as the rate of heat evolution referred to the fraction of Portland cement within the blended cement. The heat evolution (dQ/dt) is plotted as a function of the time of hydration (t). LS is an abbreviation of limestone, with 20LS-10CLS_{9N fine} representing the blended cement containing 20 wt% limestone and 10 wt% CLS_{9N fine}.

5.2.3 Compressive strength

The early compressive strength of the blends containing two SCMs reflects the setting behavior just described. The blends containing limestone as the sole SCM, i.e., blends with $P/(P+L) = 0$, show 1 and 2 days strengths larger than the blends containing only the pozzolans of Table 4.1. The 1 and 2 days strength of the Portland limestone cements are 10-15% points larger than for the pozzolan cements. Considering the inert filler the difference is 20-25% points. An intermediate strength is found for the samples with $P/(P+L) = 0.33$ and 0.67 (Figure 5.2).

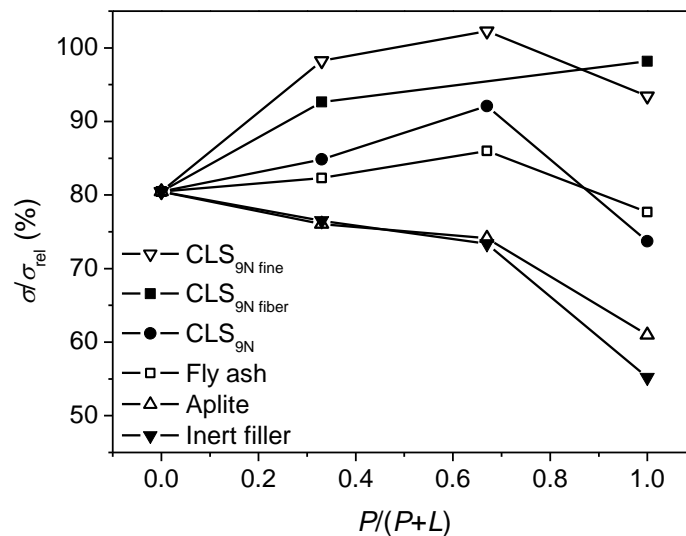


Figure 5.2: Relative compressive strength (σ/σ_{rel}) of the mortars containing different SCMs as a function of $P/(P+L)$. P is the content of pozzolan (including the inert filler) and L is the content of limestone in wt%. The solid lines are guides for the eye.

After 90 days of hydration the behavior is markedly changed for the mortars containing pozzolans participating in the strength giving reactions and, a synergy effect is found between the limestone and the pozzolan. Thus, the samples containing both limestone and pozzolan exhibit significantly higher strengths than would be predicted from the individual contributions of each constituent. This means that a synergetic effect is observed between limestone and the pozzolan. According to Figure 5.2 this is valid both for the fly ash and the two CLS_{9N} samples of various surface areas. CLS_{1N} containing mortars exhibit the same trend (Figure 5, Paper V). For CLS_{9N} fine the compressive strength of the sample containing 20 wt% of the glass and 10 wt% limestone even exceeds that of the pure cement reference, i.e., $\sigma/\sigma_{rel} > 100\%$. Due to a limited amount of fiber sample, it has not been possible to obtain a data point at $P/(P+L) = 0.67$ for that sample. A tendency towards the synergetic behavior being larger for the CLS particles than for fly ash containing blends is observed from Figure 5.2. The origin of this synergetic effect is investigated in greater detail in section 5.3.

In contrast, this synergetic effect where the strength of the samples containing two SCMs exceeds that of the blends containing only one SCM is not observed for the aplite and inert filler containing blends.

5.2.4 Summary

The mortars based on blended cements containing both CLS glass particles and limestone exhibit acceptable workability, setting behavior and early compressive strength compared to pure cement. Regarding the late compressive strength a synergetic effect is observed between the limestone and the pozzolan with strengths exceeding that predicted from blends containing just one of the constituent. For the CLS glass of high surface area ($629 \text{ m}^2/\text{kg}$) the 90 days strength of the blend containing 20% glass and 10% limestone even exceeds that of the pure cement reference. Blended cements containing mixes of CAS glass and limestone thus provides a qualified alternative to the traditional SCMs regarding mortar workability and compressive strength.

5.3 Hydration behavior

To clarify the origin of the synergetic behavior observed between the CLS glass particles and limestone within blended cements containing both materials, the hydration behavior is investigated in greater detail by means of paste samples. As for the examination of paste containing just one SCM, only pastes based on $\text{CLS}_{9\text{N fine}}$ are prepared. Pastes with $P/(P+L)$ ratios of 0, 0.33 and 1 are examined. Here the sample with $P/(P+L) = 1$ corresponds to the sample investigated in the previous chapter (section 4.2). Investigations by means of ^{29}Si MAS NMR spectroscopy, XRD and thermal analyses including the experimental conditions are described in Paper VII.

5.3.1 Identity of hydration phases formed after 90 days of hydration

As for the cements containing just one SCM the cement in the pastes under investigation in this chapter are according to Paper VII concluded to be almost fully reacted after 90 days of hydration. The glass reactivity is estimated to be 50%. The reactivity of cement components (alite and belite) and that of the glass is determined from deconvolution of ^{29}Si MAS NMR spectroscopic resonances in Paper VII. The fraction of limestone participating in the hydration reactions is in Paper VII quantified from thermo gravimetric analyses. For the blended cement containing limestone as the sole SCM it is $\approx 9\%$, whereas it for the cement containing both limestone and $\text{CLS}_{9\text{N fine}}$ ($P/(P+L) = 0.33$) is $\approx 16\%$.

Based on these results the location of the reactive mixes participating in the formation of hydration phases is plotted in the CAS (H) sub-ternary phase diagram (Figure 5.3). The composition of the Portland limestone cement is due to the low limestone reactivity just slightly shifted towards a higher CH content as compared to OPC. For comparison the figure also contains the compositional location of the

reactive mix of the blended cement containing 30% $CLS_{9N \text{ fine}}$. The reactive mix of the blended cement containing 10% $CLS_{9N \text{ fine}}$ and 20% limestone is also positioned within the same phase field as OPC with expected formation of CH, C-S-H, C_3A hydrates, iron oxide and pore solution.

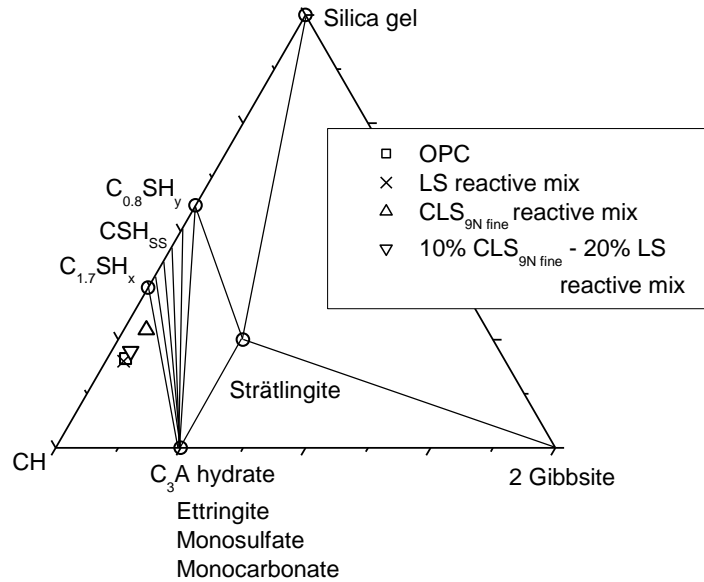


Figure 5.3: CAS (H) sub-ternary phase diagram (mol%) showing the location of the reactive mixes of the blended cements containing either 30 wt% limestone (LS), 30 wt% $CLS_{9N \text{ fine}}$ or a combination of both (10% $CLS_{9N \text{ fine}}$ and 20% LS). In addition, the location of OPC is shown in the diagram. Besides the phases predicted by the phase diagram, iron oxide and pore solution are present in excess, i.e. plotting outside the phase diagram.

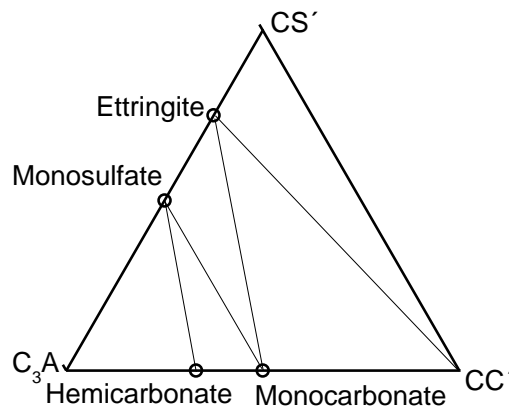


Figure 5.4: Ternary subsystem C_3A - CS' - CC' in limestone containing Portland cement system. $S' = SO_3$ and $C' = CO_2$.

The introduction of an additional component in the limestone containing cements namely CO₂ is expected to give an additional equilibrium hydration phase. As indicated on Figure 5.3 the C₃A hydrate forms a sub-system with CaSO₄ and CaCO₃. This subsystem is illustrated in Figure 5.4 with ettringite, monosulfate, hemicarbonate (C₃A-½CC'-½CH-H₁₂)² and monocarbonate (C₃A-CC'-H₁₂) as possible binary solid hydration phases.

Table 5.1 gives the hydration phases identified by means of XRD in the two limestone containing cements after 90 days hydration. In addition to the phases formed in OPC, monocarbonate and calcite are identified for the blended cement containing 30% limestone. The XRD pattern (Figure 1, Paper VII) reveals large amounts of unreacted calcite to be present. This is in correspondence with the low degree of reactivity, i.e. ≈9%, determined by thermal analyses. The simultaneous existence of monosulfate (however in small amounts) and calcite suggest that equilibrium is not reached after the 90 days of hydration (Figure 5.4). For the blended cement containing both limestone and glass the CO₂ is again incorporated into a monocarbonate phase. Large amounts of unreacted calcite are identified in agreement with the reactivity of ≈16% determined by thermal analyses. No monosulfate is identified for this sample but a carbonate containing magnesium aluminate hydrate (hydrotalcite) is identified in small amounts.

Table 5.1: Solid hydration phases identified by means of XRD after 90 days of hydration.

Hydrate phases	30% limestone	20% limestone, 10% CLS _{9N} fine
Portlandite	X	X
C-S-H	X	X
Monosulfate	X	
Ettringite	X	X
Monocarbonate	X	X
Calcite	X	X
Hydrotalcite ^a		X

^a Mg₆Al₂(CO₃)(OH)₁₆·4H₂O

Identification of hydration phases by SEM-EDS

Figures 5.5 and 5.6 show the Al/Ca ratios as function of the Si/Ca ratios for approx. 1200 SEM-EDS spot analyses on each of the two limestone containing pastes. Most of the analysed data cluster around the line representing mixtures of CH/CaCO₃ and C-S-H. It should be noticed that CH and CaCO₃ cannot be distinguished in this type of plot. A comparison of the figure with those of the pastes not containing limestone (Figures 4.7 and 4.8) shows as expected a higher fraction of spots in the CH/CaCO₃ rich region.

² C' denotes CO₂

For the paste containing both limestone and CLS_{9N}, data points are also observed on a line towards the composition of unreacted glass suggesting this to be present in the sample. The rather low glass content in this sample compared to the sample containing CLS_{9N} as the only SCM is reflected by the significantly lower abundance of points in this area compared to Figure 4.8.

Plots of S/Ca ratios as function of Al/Ca ratios indicate that less monosulfate and more ettringite are present in the samples containing limestone (Appendix B, Figure B.6 and B.7) than in OPC and the sample containing 30 wt% glass (Figure B.1 and B.2, Appendix B). This is in agreement with the expected conversion of monosulfate to monocarbonate, which also releases sulfate for formation of additional ettringite.

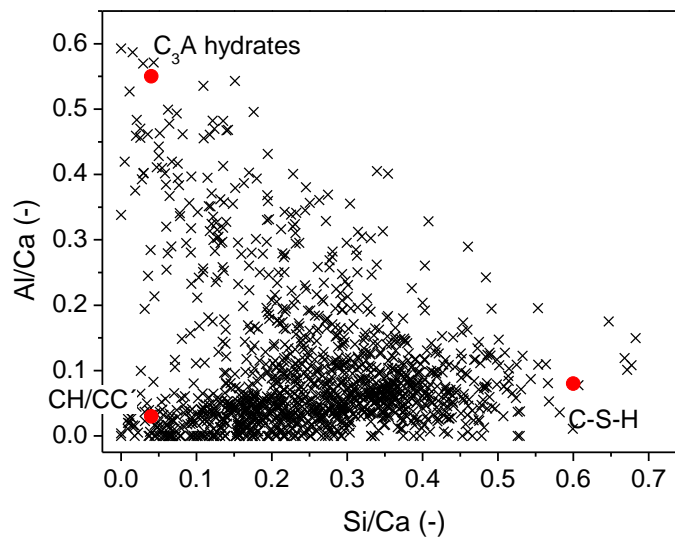


Figure 5.5: Al/Ca ratios as a function of Si/Ca atomic ratios for EDS spot analyses based on spectral imaging of a Portland limestone cement paste containing 30 wt% LS and hydrated 90 days. The atomic ratios of the hydration phases of OPC are adapted from (Odler 2007).

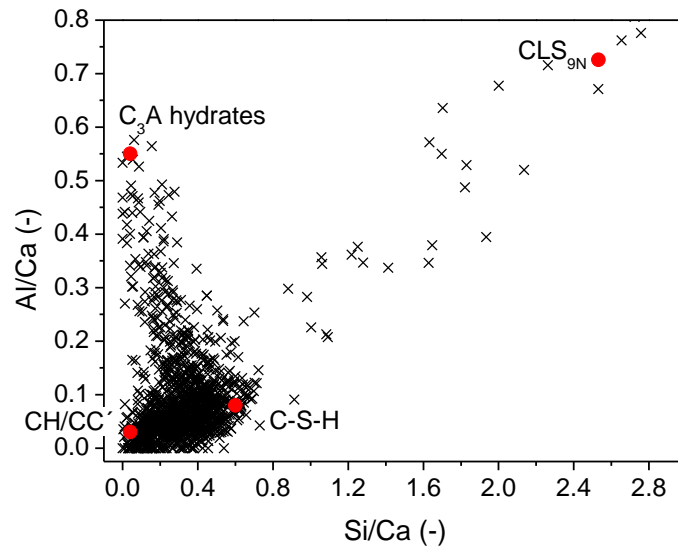


Figure 5.6: Al/Ca ratios as a function of Si/Ca atomic ratios for EDS spot analyses based on spectral imaging of a blended cement paste containing 20 wt% LS and 10 wt% CLS_{9N} fine and hydrated 90 days. The atomic ratios of the hydration phases of OPC are adapted from (Odler 2007). CLS_{9N} marks the composition of the unhydrated CLS_{9N} glass.

5.3.2 Reactivity of anhydrous clinker minerals and glass

The consumption of alite and belite as a function of time is for the blended cement containing limestone as the only SCM and for that containing both limestone and CLS_{9N} similar to that described in section 4.2.3 for the 30% CLS_{9N} blended cement. The final belite consumption is however larger with a reactivity of 80% after 90 days of hydration as compared to 65% for the 30% CLS_{9N} cement (Figure 6, Paper VII). No significant differences are observed in the course of glass consumption for the two CLS_{9N} containing blended cements during the first 28 days of hydration. A tendency towards the glass of the mix containing both glass and limestone reaching a lower degree of reactivity after 90 days compared to the sample containing only glass is however found. This difference is believed to be due to the rather difficult task of deconvoluting the glass part of the ²⁹Si NMR resonances. The uncertainty associated with quantification of remaining glass is largest for long durations of hydration, as these samples contain the smallest quantities of glass (Figure 7, Paper VII). The 90 day reactivity of the glass is for both glass containing samples approximated to be 50%.

5.3.3 Synergetic effect

Based on the results presented in the previous sections, the following conclusions can be drawn regarding the origin of the synergetic effect observed for the blended cements containing both limestone and CLS_{9N}.

The fraction of limestone participating in the formation of hydration phases is increased from 9 to 16% as the limestone is combined with CLS_{9N} in the same blended cement. A larger fraction of the limestone is thus reacting chemically in the cements containing both limestone and glass. Hence, it is possible to exploit the combined effect of limestone both as a physical filler and as a chemically reacting pozzolan to a greater extent when CLS_{9N} particles are also present in the blended cement.

As explained in section 5.1 the CaCO₃ is slowly dissolved in the pore solution reacting with any monosulfate formed. This results in the formation of a C₃A-CC'-12H phase, i.e., monocarbonate. As CaCO₃ is present in large excess for these investigations, the formation of monocarbonate is primarily depended on the C₃A content. The Al₂O₃ content is increased as CLS_{9N} is mixed with the cement predicting a larger amount of C₃A to be formed (Figure 5.3). Assuming 50% reactivity of the glass, the Al₂O₃ content is increased with approximately 0.3 g per 100 g blended cement for the cement containing 10% glass and 20% limestone compared to the sample containing only 30% limestone. This is in correspondence with the increased limestone reactivity corresponding to ≈0.45 g per 100 g blended cement ($M(\text{CaCO}_3) = 100 \text{ g/mol}$ $M(\text{Al}_2\text{O}_3) = 102 \text{ g/mol}$). Thus it seems reasonable to expect the increased Al₂O₃ content to be the reason for the observed synergy effect. Figure 5.2 furthermore reveals the 90 days compressive strength to be largest for the blended cement containing 20% glass compared to that containing only 10%. This is in agreement with the higher Al₂O₃ content of the reactive mixture of this sample. The same explanation is valid for the cements containing both limestone and fly ash. Based on the 90 days strength measurements (Figure 5.2) the synergy effect of the fly ash containing cement is found to be less than for the CLS containing cement despite the significantly larger Al₂O₃ content in fly ash (≈25 wt%) compared to the CLS glass (≈12 wt%). Considering the reduced reactivity of fly ash found by ²⁹Si NMR (Poulsen, Jakobsen & Skibsted 2009) the Al₂O₃ available for formation of hydration phases is reduced for the fly ash containing cement compared to the CLS glass containing cement. No synergetic effect is observed for the samples containing both limestone and aplite otherwise having an Al₂O₃ content of ≈10 wt%. The crystallinity of aplite makes the Al₂O₃ unavailable for pozzolanic reactions.

In addition, the conversion of monosulfate to monocarbonate releases sulfates resulting in the formation of more ettringite. This is also expected to contribute to lower porosity and higher strength.

Any incorporation of Al dissolved from the glass into the C-S-H phase will reduce the content of Al₂O₃ available for formation of monocarbonate phase. Incorporation of Al in the C-S-H phase will require absorption of alkali ions for maintaining charge neutrality. This results in an expected increase of the capacity of the C-S-H to incorporate alkali.

5.4 Summary

The introduction of both limestone and CLS_{9N} glass to the same blended cement results in a synergy effect with late strengths larger than expected from the results of the cements containing just one SCM. The increased Al₂O₃ content of the CLS containing cement compared to those not containing glass is expected to cause a larger fraction of the limestone to react chemically forming strength giving hydration phases. In this way, the combined effect of limestone as a physical filler and the pozzolanic effect of both the limestone and the CLS glass can be exploited to a greater extent.

Late strength even exceeding that of OPC is observed for the blended cement containing 20% CLS_{9N} fine and 10% limestone. Workability and early strength development of the cements containing both limestone and CLS glass is similar to the behavior of the blends containing just glass.

6 CO₂ reduction using blended cements

The previous two chapters dealt with the hydration behavior and physical performance of blended cements containing the newly developed calcium aluminosilicate based SCMs. Based on these investigations the CLS glasses are concluded to be a qualified alternative to the traditional SCMs. Equally as important is it to be able to significantly reduce the CO₂ emission from cement production by partly substituting the clinker with the CLS glass particles. Using the present production technology 800 kg CO₂ is on average released producing one tonne cement. The majority of this, i.e. 500-550 kg CO₂ per tonne clinker, is released directly from the CaCO₃ sources accounting for 80-85 wt% of the raw materials. The other major contributor is the burning of mainly fossil fuels to reach the temperatures of production. This accounts for 250-300 kg CO₂ per tonne clinker. In addition, minor CO₂ contributions are introduced from transport and from the use of electricity e.g. to run the mills used to grind the clinker. These account each for less than 5% of the total CO₂ release (World Business Council for Sustainable Development 2009, Worrel et al. 2001, Damtoft et al. 2008).

Similar to the production of cement, glass making is a highly energy intensive process taking place at elevated temperatures. Normally, the production of glass involves five main processes; mixing, melting, forming, annealing, and finishing. The major energy consumption takes place during melting within the glass furnace (Edgar et al. 2008, Sardeshpande, Gaitonde & Banerjee 2007). In the initial part of this work the composition of the glass has been optimized to reduce this energy consumption e.g. by ensuring the possibilities of working at a relatively low production temperature and achieving a glass by air cooling instead for quenching in water. In addition, the use of CAS glass as SCMs sets no requirements to homogeneity, shaping, release of stresses in the glass, etc. The processes of forming, annealing and finishing can thus be cut down compared to normal glass production of e.g. flat glasses for windows or container glasses. Importantly, the residence time within the furnace can also be significantly reduced compared to production of these materials (Beerkens 2004). Similar to cement production, CaO is introduced to the CAS glasses using limestone as the raw materials source. Hence, raw materials CO₂ release due to calcinations of carbonates must also be considered for the glass production.

6.1 CO₂ release from fuels

Soda-lime-silica glass is by far the most commonly used glass e.g. for windows and glass containers and is normally produced at 1500-1600°C. An efficient continuously operated glass melting tank producing up to several hundreds of tons of glass per day at these temperatures has a specific energy consumption of 4 GJ per ton glass produced (Edgar et al. 2008, Sardeshpande, Gaitonde & Banerjee 2007). From investigations of glass characteristics (section 3.2.1) it is found that the CAS glasses

based on natural mineral sources (the CLS glasses) can be produced at 1300-1350°C corresponding to a temperature reduction of $\approx 15\%$ compared to production of normal soda-lime-silica glass.

Normally, the heat of reactions accounts for no more than 25% of the total energy consumption during glass melting. For the CLS glasses, the heat of reactions is made up of contributions from two processes, i.e. the calcinations of limestone and the melting. In Paper II the enthalpy of calcination is for CLS_{9N} found to be 325 kJ/kg of glass whereas the melting enthalpy is estimated to ≈ 500 kJ/kg. This corresponds to approx. 20% of the total energy requirement for the production process. For comparison the enthalpy of formation of one kg of Portland clinker is approximately 1750 kJ, with the endothermic calcinations of limestone dominating this overall enthalpy (Taylor 1997).

Two of the major energy requirements during glass manufacture are the heat carried by the glass and flue gas, respectively. A large fraction of this energy can however be recovered and reused in the process e.g. to preheat the combustion air. Another important energy consumption process is the losses through walls and openings. This heat cannot be recovered and depends to a large extent on the operating temperature of the furnace (Sardeshpande, Gaitonde & Banerjee 2007, Conradt 2007, Conradt 2000). Using the method of Paper II it is estimated that the wall losses can be reduced with more than 40% reducing the operating temperature of the furnace from 1550°C to 1300°C. Assuming that the wall losses account for 15% of the total energy consumption of the furnace this reduces the specific energy consumption to ≈ 3.7 GJ/ton. According to section 1.1 this is equal to the global weighted average energy consumption for clinker production. Converting this to CO₂ equivalents assuming natural gas as the energy source for glass production, results in a CO₂ release of 250 kg per ton glass produced. Assuming coal as the energy source with 15% of alternative fuels not giving rise to any CO₂ emission, the result is a total CO₂ release of 290 kg per ton glass. This is in agreement with the size of the fuel-derived CO₂ release expected for cement production.

Comparing the fuel-derived CO₂ release of the blended cements containing CLS glasses to that of cements containing conventional clinker replacements materials such as fly ash and limestone, it is important to notice that the use of these conventional materials does not cause any fuel-derived CO₂ emission linked to cement production. Figure 6.1 shows the fuel-derived CO₂ release from the production of blended cements containing either 30 wt% CLS glass or 30 wt% fly ash or limestone. Equal fuel-derived CO₂ releases of 275 kg per ton materials produced is used for production of both CLS glasses and OPC.

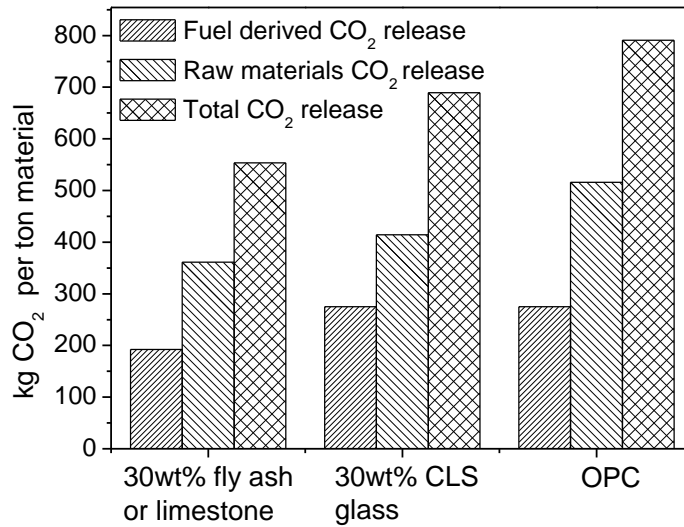


Figure 6.1: CO₂ release from production of blended cement containing 30 wt% alternative materials, i.e., either fly ash/limestone or CLS glass. In addition, the figure gives the CO₂ release of ordinary Portland cement (OPC) manufacture.

The grindability of cement clinker and the CLS_{9N} glass is furthermore compared in section 3.2.1. Here it is concluded that to obtain particles of cement fineness (575 m²/kg of the cement used in this project) less energy is required grinding the glass compared to the cement. The energy requirement and thus CO₂ release linked with grinding is thus less for the glass compared to the cement.

6.2 CO₂ release from raw materials

Limestone constitutes approximately one third of the raw materials for production of the CLS glasses. This results in the release of 175 kg CO₂ per ton glass directly from calcinations of the raw materials. This is significantly reduced compared to the production of OPC that gives rise to the release of 516 kg CO₂ per ton cement of the composition stated in Table 2.2. As the conventional SCMs as fly ash are industrial by-products no raw materials CO₂ release is linked to the cement industry using these materials. The situation is similar using limestone as a partial clinker replacement material as this is mixed with the cement subsequent to the burning process. Figure 6.1 compares the raw materials CO₂ release of blended cements containing either 30 wt% CLS glass or 30 wt% fly ash, limestone etc. with that of OPC. The raw materials CO₂ release is significantly reduced for both blended cements relative to OPC. ≈360 kg CO₂ is release per ton blended cement containing limestone or fly ash whereas ≈415 kg CO₂ is released per ton using CLS glass as SCM.

Figure 6.1 shows in addition the total CO₂ release for the three types of cements. 30% less CO₂ is emitted adding 30 wt% of the conventional waste material SCMs or limestone compared to the production of OPC. On the other hand, the use of the newly developed CLS glass particles results in a reduction of the CO₂ release of 13% compared to the pure cement.

6.3 CO₂ release relative to cement performance

A more meaningful measure of the CO₂ release of the blended cements is the CO₂ release relative to the performance of the material. A plot illustrating this is shown in Figure 6.2. Here the total CO₂ release as described above (m_{CO_2} in kg) is normalized by the 90 days compressive strength of the given cement (σ in M Pa). Figure 6.2 compares m_{CO_2}/σ for the different blended cements relative to that of pure cement as a function of the $P/(P+L)$ ratio. If $(m_{\text{CO}_2}/\sigma)_{\text{rel}} < 1$ the CO₂ per mechanical performance is reduced for the blended cement compared to the pure cement. From the figure it is concluded that if CLS_{9N} is used as the only SCM it must be ground to a rather large surface area in order to obtain reductions in the CO₂ emission without having to increase the cement fraction per cubic meter of the concrete or mortar. Grinding the CLS_{9N} glass particles to a surface area of 629 m²/kg it is possible to reduce the CO₂ release with almost 10% for the same 90 days strength. Combining both limestone and CLS_{9N} in the same cement, reductions in CO₂ emission of up to slightly above 20% can be reached. Regarding the CO₂ release from production, the CLS glasses provides a promising alternative to the limited sources of traditional SCMs.

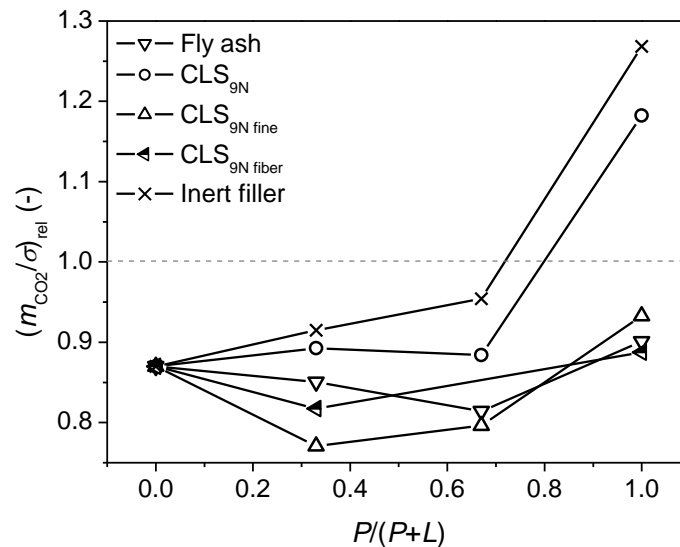


Figure 6.2: Relative raw materials CO₂ emission $(m_{\text{CO}_2}/\sigma)_{\text{rel}}$ as a function of $P/(P+L)$. $(m_{\text{CO}_2}/\sigma)_{\text{rel}} < 1$ indicates blended cements with a reduced CO₂ emission relative to the mechanical performance compared to pure cement. This limit is indicated by the dashed grey line.

7 General discussion and perspectives

According to the World Business Council for Sustainable Development 2009, clinker substitution is a potential method for reducing the massive quantities of CO₂ released from manufacture of cement. This requires the availability of large amounts of SCMs. Traditionally, industrial by-products such as fly ash, blast furnace slag and micro silica have been used for this purpose. This is a good solution, as it in addition to lowering the clinker content solves the problem of getting rid of significant amounts of waste materials. The availability of these materials is however limited and as mentioned in section 2.2 they are today almost fully utilized in Western Europe. Furthermore, the supply of such waste materials is expected to be reduced in the future. This sets up challenges for the cement industry if it wants to be able to meet the increasing future demand for cement while at the same time reduce its CO₂ emission.

For a new material to be a qualified SCM it must meet several types of criteria, some of which are listed here:

- 1) It should possess cementitious reactivity when mixed with the cement without altering important properties such as increasing the water demand. This is important to ensure acceptable performance of the final mortar or concrete.
- 2) To avoid facing the same challenge as for the traditional materials it must be available in large quantities.
- 3) The use of this material should result in a significant reduction of the CO₂ release linked to cement production.
- 4) The manufacture of blended cement containing the new SCM should be economically viable.

In this work, calcium aluminosilicate (CAS) based glass particles of compositions stated in Table 3.1 are investigated for use as SCMs. In this approach the glasses referred to as CLS glasses are produced particularly for the use as SCM. Regarding the first requirement, the addition of 30 wt% of the newly developed CLS glasses to an OPC mix slightly increases the workability of the fresh mortar. The water demand is thus not increased. This is an advantage compared to the calcined clay based SCMs tested in another part of the FUTURECEM project. Reduced early strengths are observed using the CLS glasses, whereas the blended cements show 28 and 90 days strengths approaching the strength of OPC.

To meet the second requirement it is chosen to produce the glasses using raw materials available locally and in large quantities. Similar raw materials as used for conventional PC manufacture is used for production of the glasses.

The composition of the glasses is furthermore optimized to reduce the CO₂ emission from production. Optimizations are made in regard to both the raw materials CO₂

release and the fuel-derived CO₂ release. It is estimated that the glasses can be produced emitting approximately 40% less CO₂ compared to OPC production.

Regarding the economical viability of producing the blended cements several factors, which are beyond the scope of this work, must be considered. These include a balance between the costs of establishing and maintaining facilities for glass production and the cost savings from emitting less CO₂ and thus spending less CO₂ quotas. This might leave the cement industry with the opportunity of disposing of unused CO₂ quotas. As a first step to ensure an economically reasonable production of the blended cements, it is as part of this work chosen to use low cost and locally available raw materials for glass production.

As mentioned in section 4.1.4, similar strength development patterns are found for the blended cements containing either 30 wt% CLS glass or 30 wt% fly ash (surface area of $\approx 350 \text{ m}^2/\text{kg}$). These two SCMs are however different when comparing the CO₂ releases. As fly ash and the other conventional SCMs are industrial by-products, they can directly be used in the cement industry, and hence, do not cause additional CO₂ release like CLS glasses, production of which releases CO₂. Due to the insufficient resources of these waste products, however, we have to think about an alternative way to obtain SCMs, e.g., by producing SCMs although this causes a production related CO₂ emission. Nevertheless, the overall CO₂ emission will be reduced by using the CLS based SCMs.

Another clinker replacement material not causing any production related CO₂ release is limestone. When using limestone for this purpose it is directly added into the clinker without calcination. Addition of 30 wt% limestone to the OPC results in 90 days strength reaching 80% of the pure cement strength. This is due to the combined effect of the very fine limestone particles ($1288 \text{ m}^2/\text{kg}$) acting as physical filler and the $\approx 9\%$ of the limestone taking part in the formation of hydration phases. Limestone is thus a promising clinker replacement material. It is cheap and available in large quantities near the cement producing facilities.

Generally during glass production of e.g. soda-lime-silica glass, cullet is added during the melting process to reduce the energy consumption. For instance the use of cullet significantly reduces the duration of the fining process required to obtain a homogenous glass melt. As the homogeneity is not of great concern for the positive performances of glass when mixing with cement, the addition of cullet is not considered for the production of the glasses used in this project. Instead any available waste glass, i.e., container glass, window glasses or inorganic residues from incineration of glass fiber reinforced composite materials, could be mixed with the glass after production, e.g., during the grinding process. Following this approach no energy is spent on re-melting the cullet. Dependent on the type and amount of waste glass, compositional adjustments could be made during production of the CAS glass varying the proportions of the mineral raw materials. Normal soda-lime-silica glass is not considered as the basic composition for the SCM glasses, as this in general

have a very low Al_2O_3 and rather high alkali oxide contents. Available Al_2O_3 turned out to have significant impact on the synergy effect found between the CLS glasses and limestone.

In addition to the blended cements containing one SCM, cements combining both the CLS glass particles and limestone are examined in this work. For these blended cements, a synergy effect with late strengths exceeding the ones predicted from the cements containing just one of the alternative materials is observed. This effect is caused by the relatively high Al_2O_3 content of the glass, which results in an increase of the limestone fraction reacting chemically and thus contributes to the formation of strength giving hydration products. As the addition of limestone does not result in any production related CO_2 release linked to cement production, the addition of both limestone and CLS glass to the same cement significantly reduced the final CO_2 release. Combining limestone and finely ground CLS glass in the same cement reduction in the CO_2 emission slightly above 20% can be reached for the same 90 days strength as the OPC. To elaborate the understanding of the synergy effect between limestone and pozzolans containing available Al_2O_3 in larger contents than found in the cement, additional examinations of hydration behavior should be performed. For that purpose calcium aluminosilicate glasses with systematic variations of the Al_2O_3 content should be produced, mixed with limestone, cement and water and analyzed e.g. by means of thermal analyses after various durations of the hydration process. The hydration period could beneficially be extended beyond 90 days.

An interesting observation during investigation of the performance of the blended cement mortars is the effect of increasing the surface area of the glass particles in comparison to an increasing structural disorder and hence enthalpy of the glass. On a short time scale, observable from measurements of the evolution of heat during the first 18 hours of hydration, an increasing deviation from equilibrium conditions is found to enhance the reactivity of the glass whereas an increased surface area does not show any impact (Figure 4.4). On a longer time scale, evaluated by means of compressive strength, the situation is opposite (Figure 4.5). This gives indications of the reaction mechanism. In general, the glasses show little reactivity during the first 4 days of hydration (Paper VII). Hence, the surface area and thus the number of sites available for dissolution of the glass do not impose a limiting factor on the glass reactivity. Decreased glass stability with a structure further from equilibrium conditions on the other hand eases the breakage of bonds during the initial reactions thus increasing the reactivity of the fast cooled glass particles. As the OH^- concentration in the pore solution increases as a function of time (Gartner, Tang & Weiss 1985, Thomas, Double 1981), the reduced stability of the glass becomes of minor importance. And as the glass starts to participate more in the hydration reactions with significant amounts of glass being depolymerized, the number of available sites for reaction at the surface starts to have an impact on reactivity. ^{29}Si NMR investigations of paste samples containing glass of different surface areas and

with varying degrees of structural disorder could be made to elucidate these mechanisms further.

In addition to the properties of the blended cements investigated in this work, the long term characteristics and durability of concrete based on the blended cements are also of great importance. Characteristics such as chloride penetration and corrosion of reinforcement material as well as susceptibility to sulfate attack should be investigated before final conclusions on the usage of the calcium aluminosilicate glass based SMCs can be drawn. Generally, the addition of SCMs to cement decreases the permeability possibly due to the consumption of portlandite to form additional C-S-H. Low permeability will reduce the inward diffusion of chloride and sulfate which in turn might reduce the risk of deleterious reactions caused by these ions (Taylor 1997). If this is also the case for blended cements containing the CLS glasses will however have to be examined experimentally.

As mentioned in chapter 4, high contents of alkali in the pore solution might cause alkali-silica reactions to occur in concrete exposed to moisture. As CLS_{9N} is relatively rich in alkali it is of importance to establish whether or not there is an increased risk of expansion and crack formation in the concrete due to alkali-silica reactions. This could be established by determining the content of alkali in pore solution. This might however not be straightforward as the measurement must be made after relatively long hydration to ensure significant reactivity of the glass. This will complicate the collection of pore solution from prisms as the content hereof diminishes over time. Mortar bar expansion tests could also be performed as this is a more direct method to determine the degree of expansion.

Prior to use of the CAS based SCMs in larger scale concrete production, experiments must be made regarding large scale production of the glass. This includes design of the furnace and optimization in order to reduce the energy consumption during production. It is of importance to examine possibilities for the casting process to ensure sufficiently fast cooling conditions to avoid crystallization. Within this work, two portions of glass melts of approximately 8 kg each have been made using a 5 liter silicon carbide/graphite crucible. For these glass preparations the melt was casted tilting the crucible thus pouring the melt unto a steel plate. The melt was spread on the plate by hand using long steel tools. This casting method provided sufficiently fast cooling to avoid crystallization of the melt. The glass produced in this test will be used to investigate the formulation and mixing of concrete using blended cements containing 30 wt% of the glass. The preliminary results indicate that concrete mixes can be made without changing the precipices used for the OPC based concrete. This is also an important characteristic of the CLS glasses.

8 Conclusions

The aim of the present study is the development of innovative supplementary cementitious materials based on calcium aluminosilicate glasses. The incentive to produce such materials specifically for the use as SCM is that the availability of the traditional by-product based SCMs such as fly ash and blast furnace slag is insufficient to meet the future requirements from the cement industry. This is especially a problem in regions like Western Europe.

The objective of this work has been: 1) to design a glassy system with a composition optimized for the use as SCM, and 2) to examine the physical performance of cement mortars as well as hydration behavior of pastes containing these newly developed glass particles.

The glass composition has been optimized regarding three main requirements:

- To ensure a future economical viable production and to avoid the problem of insufficient availability of the SCMs, the glass should be based on low cost raw materials available locally in large quantities. Hence it is chosen to base the glass on the conventional raw materials used for cement production, i.e., clay, limestone and sand, however mixed in proportions different from cement.
- The production of the glass should give rise to a significantly reduced CO₂ emission compared to the production of Portland cement. The glass composition is thus adjusted to ensure both low raw materials CO₂ emission and low fuel-derived CO₂ emission. The amount of CO₂ released from raw materials is directly linked to the CaO content of the glass, as the CaO is provided by addition of limestone. For the CLS glasses ≈ 175 kg of CO₂ is released per tonne glass produced. This accounts for around one third of the 516 kg of CO₂ released producing one tonne of the OPC used in this work. Acceptable fuel-derived CO₂ release can be ensured by adjusting the composition to obtain a relatively low practical melting temperature thus allowing for the use of a correspondingly low furnace operating temperature. The CLS glasses can be produced at 1300-1350°C which is significantly lower than the production temperature for OPC ($\approx 1450^\circ\text{C}$) as well as for common soda-lime-silica glass products (1500-1600°C). In addition, all glass melts studied in this work exhibit rather high glass forming ability thus allowing for the melts to be vitrified without forced cooling. This also contributes to maintaining the fuel-derived CO₂ at a minimum. Combining these investigations, it is estimated that the glass can be produced with comparable or slightly reduced fuel-derived CO₂ in relation to the production of cement. Using 275 kg CO₂ per tonne material as an estimate of the fuel-derived CO₂ release from production of both clinker and glass, the total CO₂

release from production of both materials can be calculated. As expected the production of cement clinker releases approximately 800 kg of CO₂ per tonne, whereas the production of CLS glass in contrast results in the release of approximately 450 kg CO₂ per tonne. The glass can thus be produced under conditions causing significantly lower CO₂ emissions than the cement.

Measurement of surface area as a function of grinding time in a porcelain mill have shown that the clinker and CLS_{9N} glass possess comparable grindability to a surface area of approximately 450 m²/kg. At surface areas larger than this, the glass show superior grindability in comparison to the clinker. Approximately 5% of the CO₂ release for cement production is due to the use of electricity, e.g. to run the mills used to grind the clinker.

- For the glass to be a useful SCM it must in addition contribute to the formation of strength giving hydration phases as it is mixed with cement. The glass should thus possess pozzolanity to ensure similar or better cement performance, resulting in acceptable concrete performance without having to increase the content of cement per cubic meter of concrete.

This is at first tested as the reactivity of the glass in a saturated Ca(OH)₂ solution. ²⁹Si and ²⁷Al MAS NMR spectroscopy is used to investigate any products formed from these reactions. It is found that dimers and chains of SiO₄ units are formed during reaction with Ca(OH)₂ and water, and that a phase containing AlO₆ units possessing a higher degree of order than in the original glass is also formed. These phases resemble the C-S-H phase and the calcium aluminate hydrates formed during OPC hydration. The calcium aluminosilicate based glass particles are thus pozzolanically active. The degree of pozzolanity is found to increase as minor components are introduced from the natural raw materials and further as additional Na₂O is introduced to the CLS_{5N} and CLS_{9N} glasses.

From investigations of these properties, the CLS glasses show promising potential as SCMs both in regard to both reduction of the CO₂ emission and ensuring acceptable performance of mortars and concretes.

To get a deeper understanding of how compositional changes affect the glass properties via alteration of the glass structure, the composition-structure relationship of the ten three component CAS glasses is investigated in section 3.1.2. Structural heterogeneity is found in the intermediate-range order with clustering of highly depolymerized regions of low Al content and highly polymerized regions of alternating SiO₄ and AlO₄ tetrahedra.

The next step of the work has been more direct investigations of the performance of blended cements containing the CLS glasses. For these investigations blended cements containing 30 wt% clinker replacements have been prepared. The physical performances of mortars are tested in relation to workability, setting behavior and

compressive strength after various durations of hydration. These investigations demonstrate:

- Standard mortar workability is slightly improved for the blended cements compared to OPC.
- The glass does not contribute to early hydration measured as the heat evolution during the first 18 hours of hydration. These measurements indicate a slightly increased duration until the onset of setting for the blended cements.
- From measurement of strength the pozzolanic reactivity of the CLS glasses is limited at early stages of hydration but increases over time. At 90 days hydration the strength reaches 75% of the OPC for blended containing CLS_{9N} with a surface area of 371 m²/kg. This increases to above 90% as the surface area of the glass is increased to 629 m²/kg. In general, the strength development is similar to that of blended cements containing fly ash.
- A synergetic effect is observed at long durations of hydration for blended cement containing both limestone and CLS glass. For these blends strengths are higher than predicted from the individual contributions of each constituent for the cases of 28 and 90 days hydration. This is due to a larger fraction of the limestone participating in formation of the strength giving monocarbonate phase as the content of Al₂O₃ available for reaction with limestone is increased by the presence of CLS glass. For blended cements containing 20% CLS_{9N fine} and 10% limestone the 90 days strength even exceeds that of OPC.
- From investigations of hydration behavior by means of ²⁹Si MAS NMR spectroscopy and XRD the glass is found to be incorporated in hydration phases similar to the once formed during hydration of OPC.

From the investigations of physical performances of the mortars containing blended cements with 30 wt% clinker substitution it is confirmed that the CLS glasses are a qualified candidate as a SCM. This is due to the fact that the usage of blended cement results in acceptable mortar performance as the clinker is substituted with glass on a 1:1 weight basis.

To get a measure of the CO₂ release relative to the performance of the blended cements, the CO₂ release of the given blended cement has been normalized with the 90 day strength. If the CAS based glasses are used as the sole SCM it must be ground to a rather large surface area in order to obtain reduction in the CO₂ release without increasing the content of cement per cubic meter of concrete. With a surface area of 629 m²/kg the CO₂ emission can be reduced by 10% for the same performance as OPC. Combing limestone and CLS glass particles in the same cement, 20% reductions can be achieved.

Thus, the use of CLS glasses as SCMs is a good approach for significantly reducing the CO₂ emission from cement production. To reach the FUTURECEM aim of reducing the CO₂ release with at least 30%, the use of CAS based SCMs must

however be combined with other approaches to reduce the CO₂. This could e.g. be a combination of the CLS glasses with clinkers optimized to show high compatibility with the CLS based SCMs.

9 List of references

- Aalborg Portland 2009, *Årsrapport 2009, Aalborg Portland*, Aalborg Portland, Cementir Holding, Aalborg, Denmark.
- Allwardt, J.R., Lee, S.K. & Stebbins, J.F. 2003, "Bonding preferences of non-bridging O atoms: Evidence from O-17 MAS and 3QMAS NMR on calcium aluminate and low-silica Ca-aluminosilicate glasses", *American Mineralogist*, vol. 88, pp. 949-954.
- Ambroise, J., Maximilien, S. & Pera, J. 1994, "Properties of Metakaolin Blended Cements", *Advances in Cement Based Materials*, vol. 1, pp. 161-168.
- Andersen, M.D., Jakobsen, H.J. & Skibsted, J. 2003, "Incorporation of aluminum in the calcium silicate hydrate (C-S-H) of hydrated Portland cements: A high-field ²⁷Al and ²⁹Si MAS NMR investigation", *Inorganic Chemistry*, vol. 42, pp. 2280-2287.
- Beerkens, R. 2004, "Modular Melting - Industrial Glassmelting Process Analysis", *American Ceramic Society Bulletin*, vol. 83, no. 4, pp. 28-32.
- Bleazard, R.G. 2007, "The History of Calcareous Cements" in *Lea's Chemistry of Cement and Concrete*, ed. P.C. Hewlett, Fourth edn, Elsevier, Oxford, UK, pp. 1-23.
- Chunxiang, Q., Hongding, G. & Xianghui, L.M., T. 1994, "Mechanism of mineral admixture suppressing alkali-silica reaction: Part II. Retardtion of the transport of Na, K and OH ions in the pore solution structure caused by acidic action of mineral admixture particles in matrix", *Cement and Concrete Research*, vol. 24, pp. 1327-1334.
- Conradt, R. 2007, "Production efficiency, environmental sustainability, and glass quality - a thermodynamic optimisation of three conflicting objectives", *Glass Technology-European Journal of Glass Science and Technology Part A*, vol. 48, no. 5, pp. 235-241.
- Conradt, R. 2000, "A generic approach to the relation between pull rate and energy consumption of glass furnaces", *Glastechnische Berichte-Glass Science and Technology*, vol. 73, pp. 252-261.

- Damtoft, J.S., Lukasik, J., Herfort, D., Sorrentino, D. & Gartner, E.M. 2008, "Sustainable development and climate change initiatives", *Cement and Concrete Research*, vol. 38, pp. 115-127.
- Duchesne, J. & Bérubé, M.A. 1994, "The effectiveness of supplementary cementing materials in suppressing expansion due to ASR: Another look at the reaction mechanisms part 2: Pore solution chemistry", *Cement and Concrete Research*, vol. 24, pp. 221-230.
- Edgar, R., Holcroft, C., Pudner, M. & Hardcastle, G. 2008, *UK Glass Manufacture - 2008 A Mass Balance Study*, 1st edn, GTS specialist knowledge in glass, Envirowise - sustainable practices, sustainable profits, UK.
- Ehlers, E.G. 1972, *The Interpretation of Geological Phase Diagrams*, first edn, W. H. Freeman and Company, USA.
- FUTURECEM Unpublished data.
- Gartner, E.M., Tang, F.J. & Weiss, S.J. 1985, "Saturation factors for calciumhydroxide and calciumsulfates in fresh Portland cement pastes", *Journal of American Ceramic Society*, vol. 68, no. 667, pp. 673-J. Am. Ceram. Soc.
- Greaves, G.N. 1985, "EXAFS and the structure of glass", *Journal of non-crystalline solids*, vol. 71, pp. 203-217.
- Greaves, G.N. & Sen, S. 2007, "Inorganic glasses, glass-forming liquids and amorphizing solids", *Advances in Physics*, vol. 56, no. 1, pp. 1-166.
- Hasholt, M.T., Hansen, H. & Thørgersen, F. 2003, *Metoder til genanvendelse af farvede glasskår til produktion af tegl og beton til vejbygning - del 1: Litteraturstudium, Miljøprojekt Nr. 819 2003*, Miljøstyrelsen, Denmark.
- Hasholt, M.T., Mathiesen, D., Hansen, H. & Thørgersen, F. 2004, *Metoder til genanvendelse af farvede glasskår til produktion af tegl og beton til vejbygning - del 2: Pilotforsøg, Miljøprojekt Nr. 889 2004*, Miljøstyrelsen, Denmark.
- He, C., Osbæck, B. & Makovicky, E. 1995, "Pozzolanic reactions of six principal clay minerals: Activation, reactivity assessments and technological effects", *Cement and Concrete Research*, vol. 25, no. 1691, pp. 1702.
- Hill, R., Wood, D. & Thomas, M. 1999, "Trimethylsilylation analysis of the silicate structure of fluoro-alumino-silicate glasses and the structural role of fluorine", *Journal of Materials Science*, vol. 34, pp. 1767-1774.

- Hjort, J., Skibsted, J. & Jakobsen, H.J. 1988, "29Si MAS NMR studies of Portland cement components and the effects of microsilica on the hydration reaction", *Cement and Concrete Research*, vol. 18, pp. 789-798.
- Hong, S.Y. & Glasser, F.P. 1999, "Alkali binding in cement pastes Part I. The C-S-H phase", *Cement and Concrete Research*, vol. 29, pp. 1893-1903.
- Humphreys, K. & Mahasenan, M. 2002, *Toward a sustainable cement industry. Sub-study 8: climate change*, An Independent Study Commissioned to Battelle by World Business Council for Sustainable Development.
- Klemm, W.A. & Adams, L.D. 1990, "An investigation of the formation of carboaluminates" in *Carbonate Additions to Cement, ASTM STP 1064*, eds. P. Klieger & R.D. Hooton, 1st edn, American Society for Testing and Materials, Philadelphia, USA, pp. 60-72.
- Krøyer, H., Lindgreen, H., Jakobsen, H.J. & Skibsted, J. 2003, "Hydration of Portland cement in the presence of clay minerals studied by 29Si and 27Al MAS NMR spectroscopy", *Advances in Cement Research*, vol. 15, pp. 103-112.
- Lawrence, C.D. 2007a, "The Constitution and Specification of Portland Cements" in *Lea's Chemistry of Cement and Concrete*, ed. P.C. Hewlett, fourth edn, Elsevier, Oxford, UK, pp. 131-193.
- Lawrence, C.D. 2007b, "The Production of Low-Energy Cements" in *Lea's chemistry of cement and concrete*, ed. P.C. Hewlett, 4th edn, Elsevier, Oxford, pp. 421-470.
- Lee, S.K. & Stebbins, J.F. 2006, "Disorder and the extent of polymerization in calcium silicate and aluminosilicate glasses: O-17 NMR results and quantum chemical molecular orbital calculations", *Geochimica et Cosmochimica Acta*, vol. 70, pp. 4275-4286.
- Massazza, F. 2007, "Pozzolana and Pozzolanic Cements" in *Lea's chemistry of cement and concrete*, ed. P.C. Hewlett, 4th edn, Elsevier, Oxford, pp. 471-635.
- Mauro, J.C., Uzun, S.S., Bras, W. & Sen, S. 2009a, "Nonmonotonic Evolution of Density Fluctuations during Glass Relaxation", *Physical Review Letters*, vol. 102, pp. 15506.
- Mauro, J.C., Yue, Y.Z., Ellison, A.J., Gupta, P.K. & Allan, D.C. 2009b, "Viscosity of glass-forming liquids", *Proceedings of the national academy of sciences*, vol. 106, pp. 19780-19784.

- Merzbacher, C.I., Sherriff, B.L., Hartman, J.S. & White, W.B. 1990, "A high-resolution ^{27}Al and ^{29}Si NMR study of alkaline earth aluminosilicate glasses", *Journal of Non-crystalline solids*, vol. 124, pp. 194-206.
- Mishulovich, A. & Hansen, E.R. 2000, "Manufactured supplementary cementitious materials", *World Cement*, , no. June, pp. 98-103.
- Mishulovich, A. & Hansen, E.R. 1996, "Manufacture of supplementary cementitious materials from cement kiln dust", *World Cement Research and Development*, , no. March, pp. 116-120.
- Muller, D., Gessner, W., Behrens, H.J. & Scheler, G. 1981, "Determination of the aluminum coordination in aluminum-oxygen compounds by solid-state high-resolution ^{27}Al NMR", *Chemical Physics Letters*, vol. 70, pp. 59-62.
- Mysen, B.O. 1990, "Role of Al in depolymerized, peralkaline aluminosilicate melts in the systems $\text{Li}_2\text{O-Al}_2\text{O}_3\text{-SiO}_2$, $\text{Na}_2\text{O-Al}_2\text{O}_3\text{-SiO}_2$, and $\text{K}_2\text{O-Al}_2\text{O}_3\text{-SiO}_2$ ", *American Mineralogist*, vol. 75, pp. 120.
- Mysen, B.O. & Richet, P. 2005, *Silicate glasses and melts - properties and structure*, 1st edn, Elsevier B. V., Amsterdam.
- Nepper-Christensen, P. 1985, "Cement" in *Beton-Bogen*, eds. A.G. Herholdt, C.F.P. Justesen, P. Nepper-Christensen & A. Nielsen, second edn, Aalborg Portland, Denmark, pp. 268-298.
- Nielsen, E.P., Herfort, D. & Geiker, M.R. 2005, "Phase equilibria in hydrated Portland cement", *Cement and Concrete Research*, vol. 35, pp. 109-115.
- Odler, I. 2007, "Hydration, Setting and Hardening of Portland Cement" in *Lea's Chemistry of Cement and Concrete*, ed. P.C. Hewlett, 4th edn, Elsevier, Oxford, UK, pp. 241-289.
- Ossi, P.M. 2003, *Disordered Materials - An Introduction*, 1st edn, Springer.
- Péra, J., Husson, S. & Guilhot, B. 1999, "Influence of finely ground limestone on cement hydration", *Cement and Concrete Research*, vol. 21, pp. 99-105.
- Poulsen, S.L., Jakobsen, H.J. & Skibsted, J. 2009, "Methodologies for measuring the degree of reaction in Portland cement blends with supplementary cementitious materials by ^{27}Al and ^{29}Si MAS NMR spectroscopy", *Proceedings of the 17th IBAUSIL - Internationale Baustofftagung*, vol. 1, pp. 177-188.

- Price, D.L. 1996, "Intermediate-range order in glasses", *Current Opinion in Solid State & Materials Science*, vol. 1, pp. 572-577.
- Ramachandran, V.S. 1988, "Thermal analysis of cement components hydrated in the presence of calcium carbonate", *Thermochimica Acta*, vol. 127, pp. 385-394.
- Ramachandran, V.S. & Chun-mei, Z. 1986, "Influence of CaCO₃ on hydration and microstructural characteristics of tricalcium silicate", *Il Cemento*, vol. 83, pp. 129-152.
- Richardson, I.G. 1999, "The nature of C-S-H in hardened cement", *Cement and Concrete Research*, vol. 129, pp. 1131-1147.
- Sardeshpande, V., Gaitonde, U.N. & Banerjee, R. 2007, "Model based benchmarking for glass furnace", *Energy Conservation and Management*, vol. 48, pp. 2718-2738.
- Schwarz, N., Cam, H. & Neithalath, N. 2008, "Influence of a fine glass powder on the durability characteristics of concrete and its comparison to fly ash", *Cement and Concrete Research*, vol. 30, pp. 486-496.
- Shayan, A. & Xu, A. 2006, "Performance of glass powder as pozzolanic material in concrete: A field trial on concrete slabs", *Cement and Concrete Research*, vol. 36, pp. 457-468.
- Shelby, J.E. 2005, *Introduction to glass science and technology*, 2nd edn, The Royal Society of Chemistry, Cambridge, UK.
- Shi, C., Wu., Y., Riefler, C. & Wang, H. 2005, "Characteristics and pozzolanic reactivity of glass powder", *Cement and Concrete Research*, vol. 35, pp. 987-993.
- Shi, C. & Zheng, K. 2007, "A review on the use of waste glasses in the production of cement and concrete", *Resources, Conservation and Recycling*, vol. 52, pp. 234-247.
- Širok, B., Blagojević, B. & Bullen, P. 2008, *Mineral Wool*, 1st edn, Woodhead Publishing, Cambridge, UK.
- Stamboulis, A., Hill, R.G. & Law, R.V. 2004, "Characterization of the structure of calcium alumino-silicate and calcium fluoro-alumino-silicate glasses by magic angle spinning nuclear magnetic resonance (MAS-NMR)", *Journal of Non-crystalline solids*, vol. 333, pp. 101-107.

- Taylor, H.F.W. 1997, *Cement Chemistry*, Academic Press, New York.
- Thomas, N.L. & Double, D.D. 1981, "Calcium and silicon concentrations in solution during the early hydration of Portland cement and tricalcium silicate", *Cement and Concrete Research*, vol. 11, pp. 675-687.
- Tsivilis, S., Chaniotakis, E., Badogiannis, E. & Pahoulas, G. 1999, "A study on the parameters affecting the properties of Portland limestone cements", *Cement and Concrete Research*, vol. 21, pp. 197-116.
- Tsivilis, S., Tsantilas, J., Kakali, G., Chaniotakis, E. & Sakellariou, A. 2003, "The permeability of Portland limestone cement concrete", *Cement and Concrete Research*, vol. 33, pp. 1465-1471.
- Varshneya, A.K. 1994, *Fundamentals of inorganic glasses*, 1st edn, Academic Press, CA, USA.
- Vuk, T., Tinta, V., Gabrovsek, R. & Kaucic, V. 2001, "The effect of limestone addition, clinker type and fineness on properties of Portland cement", *Cement and Concrete Research*, vol. 31, pp. 135-139.
- World Business Council for Sustainable Development 2009, *Cement Technology Roadmap 2009 - Carbon emissions reductions up to 2050*, OECD/IEA, World Business Council for Sustainable Development.
- Worrel, W., Price, N., Martin, N., Hendriks, C. & Meida, L.O. 2001, "Carbon dioxide emission from the global cement industry", *Annual Review of energy and environment*, vol. 26, pp. 303-329.
- Yue, Y.Z., Christiansen, J.d. & Jensen, S.L. 2002, "Determination of the fictive temperature for a hyperquenched glass", *Chemical Physics Letters*, vol. 357, pp. 20-24.
- Yue, Y.Z., von der Ohe, R. & Jensen, S.L. 2004, "Fictive temperature, cooling rate, and viscosity of glasses", *Journal of Chemical Physics*, vol. 120, pp. 8053-8059.
- Zelic, J., Krstulovic, R., Tkalcec, E. & Krolo, P. 1999, "Durability of the hydrated limestone-silica fume Portland cement mortars under sulphate attack", *Cement and Concrete Research*, vol. 29, pp. 819-826.
- Zeng, Q. & Stebbins, J.F. 2000, "Fluoride sites in aluminosilicate glasses: High-resolution ^{19}F NMR results", *American Mineralogist*, vol. 85, pp. 863-867.

A $\text{CaF}_2\text{-CaO-Al}_2\text{O}_3\text{-SiO}_2$ system

A.1 Introduction

Addition of fluorines to silicates and aluminosilicates is known to demonstrate fluxing behavior by means of lowering the viscosity (Zeng, Stebbins 2000, Stamboulis, Hill & Law 2004, Hill, Wood & Thomas 1999). Addition of fluorine in the form of CaF_2 is thus a method for lowering the practical melting temperature of silicate or aluminosilicate melts without the addition of alkali carbonates giving rise to increased CO_2 emission from the raw materials. Furthermore it is possible to reduce the amount of carbonates required to obtain a given calcium content substituting part of the CaCO_3 by CaF_2 .

In general, the reduced viscosity is believed to be caused by replacement of bridging oxygens in the glassy network with non-bridging fluorines. Several studies have reported a preference of fluorine to be linked to aluminum instead of silicon in peralkaline aluminosilicates. This is of importance as a large part of the fluorine will be lost by volatilization of SiF_4 species causing corrosion and environmental problems. If fluorine is bound to Al a significantly smaller fraction is lost by evaporation than if considerable amounts of SiF_4 were formed. In addition to replacing bridging oxygens linked to the network forming species, F-Ca(*n*) species with *n* representing the number of Ca coordinated with the fluorine is reported to be formed in calcium aluminosilicate glasses (Zeng, Stebbins 2000, Stamboulis, Hill & Law 2004, Hill, Wood & Thomas 1999).

In this work, we test the effect of using CaF_2 as the raw materials source of part of the CaO in the three component $\text{CaO-Al}_2\text{O}_3\text{-SiO}_2$ system. Based on the basis composition of CAS1, i.e. the eutectic composition of anorthite-wollastonite-tridymite, three glasses containing varying fluorine contents (2, 4 and 8 mol% CaF_2) have been synthesized. To maintain constant calcium content for all glasses, CaO was substituted with the given amount of CaF_2 during glass preparation. The main interest is to investigate the effect of fluorine addition on the practical melting temperature. Preliminary investigations of the fluorine structural role within the glassy network are also performed by solid-state ^{19}F MAS NMR spectroscopy. These investigations are used to explain the effect of fluorine addition on viscosity.

A.2 Experimental

Table A.1 states the designed compositions of the four glasses. The glasses were synthesized by melting the batch in a $\text{Pt}_{90}\text{Rh}_{10}$ crucible in a box furnace (model SF6/17 Entech, Angelholm, Sweden) in atmospheric air. The analytical chemicals SiO_2 , Al_2O_3 , CaCO_3 and CaF_2 were used for batch preparation. To get homogenized glasses, a two-step melting process was carried out. First, two glasses containing either none (CAS1) or 8 mol% CaF_2

(CAS-F₈) were melted for 2 hours at 1550°C and 1510°C, respectively. To minimize evaporation an Al₂O₃ lid was used to cover the crucible. The glasses are quenched on a graphite plate and subsequently crushed. To obtain the glasses in Table A.1 the crushed pieces of CAS1 and CAS-F₈ were mixed in the right proportions and remelted for 2 hours at 1510-1550°C depending on the CaF₂ content. The glasses were annealed at temperatures in the range 750-800°C depending on the CaF₂ content.

Table A.1: Designed chemical composition (mol%) of the fluorine containing CAS glasses.

	SiO ₂	Al ₂ O ₃	CaO	CaF ₂
CAS1	65	9	26	0
CAS1-F ₂	65	9	24	2
CAS1-F ₄	65	9	22	4
CAS1-F ₈	65	9	18	8

The viscosity (η) was measured using concentric cylinder viscometry in the temperature range from 1050°C to 1550°C under atmospheric conditions. This temperature range corresponds to viscosities of approx. 10^0 - 10^3 Pa s. The furnace was a box furnace (model HT 7, Scandiaovnen A/S, Allerød, Denmark) and the viscometer head was a Physica Rheolab MC1 (Paar Physica, Stuttgart, Germany). The viscometer was calibrated using the NBS (National Bureau of Standards) 710A standard glass.

The glass transition temperature (T_g) was determined calorimetrically using a simultaneous thermal analyzer (NETZSCH STA 449C Jupiter, Selb, Germany). T_g was found from the second upscan curve as the onset temperature of the glass transition peak using a heating rate for the second upscan of 10 K/min. This is equal to the prior cooling rate. This method for determining T_g agrees with the standard method described by (Yue, Christiansen & Jensen 2002, Yue 2008). In this work it has been utilized that at T_g the viscosity is 10^{12} Pa s.

Solid-state ¹⁹F MAS NMR spectra were recorded at 282.2 MHz on a Varian UNITY-300 ($B_0 = 7.05$ T) spectrometer using a 5 mm home-built CP/MAS probe for 5 mm o.d. rotors and a spin-echo pulse sequence to reduce spectral artefacts related to truncation of the FID. The experiments employed a spinning speed of 10.0 Hz, an echo delay of 100 μ s, a 30 s relaxation delay and a ¹⁹F rf field strength of $\gamma/2\pi = 60$ kHz. The spectra are referenced to neat CFC1₃. NMR measurements were performed on the three fluorine containing glasses as well as on a pure CaF₂ sample.

Vickers hardness (H_v) was measured by micro indentation (Duramin, Struers, Denmark). Varying loads in the range 1.96 N to 9.81 N was applied for 5 s and 15 indentations were performed for each determination of H_v .

A.3 Results and discussion

Figure A.1 shows the viscosity-temperature relation for the four melts (Table A.1). As expected the viscosity drops as the fluorine content within the melt is increased. The effect is most pronounced in the high-viscosity range. The viscosity temperature relation is described by the MYEGA equation (Mauro et al. 2009). From this description the practical melting temperature (T_{pm}) is found as the isokom temperature corresponding to a viscosity of 10 Pa s. Figure A.2 visualizes how both T_{pm} and T_g decreases as a function of the fluorine content. This confirms that the network connectivity to some extent is broken as CaF_2 is introduced to the melt. Addition of a few percentages CaF_2 is observed to significantly reduce both T_{pm} and T_g with approx. 40°C .

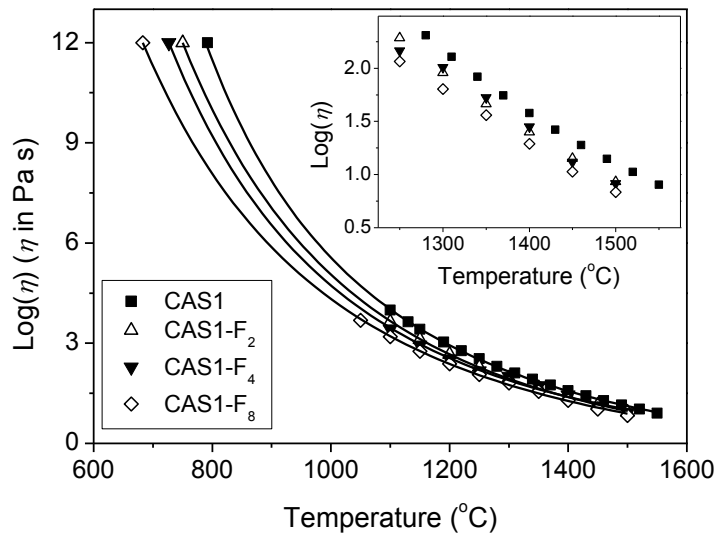


Figure A.1: Viscosity (η) given as $\log \eta$ as a function of temperature for the four glasses with varying fluorine content. The symbols represents the measured values and the solid lines are the fits of the MYEGA equation to the data. The inset shows a zoom on the low viscosity end of the plot.

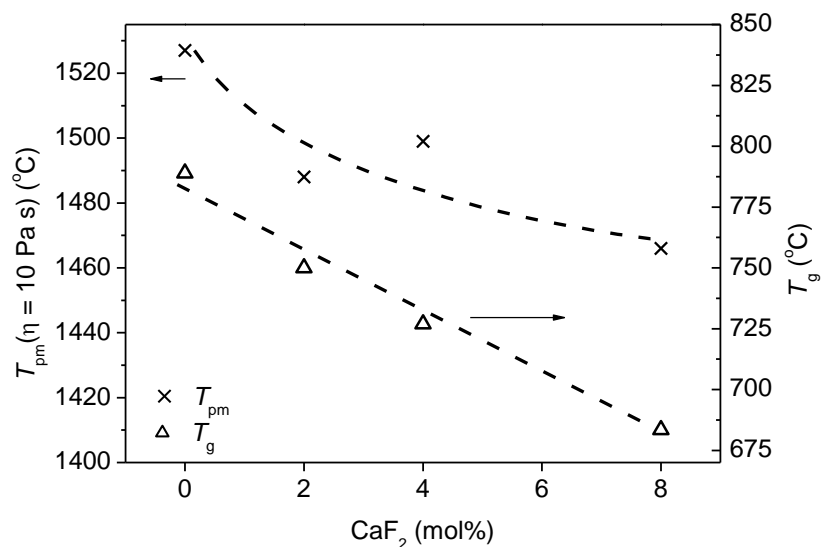


Figure A.2: Practical melting temperature (T_{pm}) and glass transition temperature (T_g) as a function of the CaF_2 content of the glasses. The dashed lines should be regarded as guides for the eye.

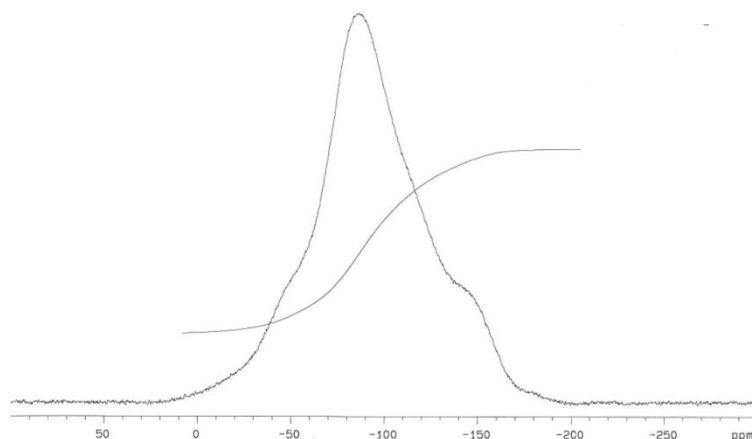


Figure A.3: ^{19}F NMR resonance of CAS-F₄. The s-shaped line represents the integration of the peak.

Similar ^{19}F MAS NMR resonances are obtained for all three fluorine containing CAS glasses. As expected the integral increases proportionally with increasing CaF_2 content. It has not been possible to determine the absolute fluorine content of the glasses as the signal intensity of the pure CaF_2 sample is significantly reduced due to strong homonuclear dipolar coupling between the ^{19}F nuclei. The resonance of CAS-F₄ is shown in Figure A.3. Broad peaks are observed at $\sim -90\text{ppm}$ and $\sim -140\text{ ppm}$. A shoulder in the high frequency side of the largest resonances suggests a third peak to be present at $\sim -50\text{ ppm}$. Based on previous

^{19}F NMR investigations on aluminosilicates the peak at -90 ppm is identified as corresponding to F-Ca(n) units whereas the peak at -140 ppm has been proven to originate from Al-F-Ca(n) species (Zeng, Stebbins 2000, Stamboulis, Hill & Law 2004). The previous authors did not observe any peaks at approx. -50 ppm. The F-Ca(n) peak is significantly larger for all samples than the Al-F-Ca(n) peak, indicating that the majority of the fluorine is present in these sites. The ratio between the intensity of the Al-F-Ca(n) and the F-Ca(n) peaks is approximately constant (0.3-0.4) for all three samples. For the pure CaF_2 sample a sharp peak at -110 ppm is observed. This corresponds with previous observations (Zeng, Stebbins 2000, Stamboulis, Hill & Law 2004). That no peak is present at this chemical shift for the glass samples confirms that the fluorine is incorporated into the glass structure and not present as CaF_2 clusters. The incorporation of fluorine in Al-F-Ca(n) species, i.e., the replacement of bridging oxygens with fluorine, explains the reduction in characteristic temperature as shown in Figure A.2. Figure A.3 however reveals that the majority of the fluorine form complexes with Ca not breaking any bridging oxygen bonds. This might however also result in more network disruption as the ability of Ca^{2+} to crosslink two NBOs is lost.

Vickers hardness measurements show a vague tendency towards decreasing hardness as a function of fluorine content (Table A.2). A reduction in the network connectivity is expected to cause a reduced hardness. That only a vague tendency is observed might be linked to the fact that the majority of the fluorine is incorporated in F-Ca(n) units not breaking any bridging oxygen bonds.

Table A.2: Vickers hardness at different loads. The results are obtained as the average of 15 indentations.

Load (N)	0 mol% CaF ₂	2 mol% CaF ₂	4 mol% CaF ₂	8 mol% CaF ₂
1.96	6.40±0.12	6.41±0.12	6.51±0.12	5.76±0.39
2.94	6.37±0.14	6.34±0.11	6.40±0.15	6.32±0.12
4.91	6.38±0.09	6.32±0.06	6.34±0.18	6.28±0.13
9.81	6.25±0.10	6.20±0.11	6.20±0.17	6.15±0.14

A.4 Conclusions

The substitution of a few percentages CaO with CaF_2 is found to significantly reduce the practical melting temperature of the calcium aluminosilicate melt. The glass melting tank can thus be operated at a lower temperature by addition of fluorine to the melt resulting in a reduced energy consumption and thus CO_2 emission. ^{19}F MAS NMR reveals the fluorine to be incorporated in the glassy network within Al-F-Ca(n) and F-Ca(n) species.

A.5 References

- Hill, R., Wood, D. & Thomas, M. 1999, "Trimethylsilylation analysis of the silicate structure of fluoro-alumino-silicate glasses and the structural role of fluorine", *Journal of Materials Science*, vol. 34, pp. 1767-1774.
- Mauro, J.C., Yue, Y.Z., Ellison, A.J., Gupta, P.K. & Allan, D.C. 2009, "Viscosity of glass-forming liquids", *Proceedings of the national academy of sciences*, vol. 106, pp. 19780-19784.
- Stamboulis, A., Hill, R.G. & Law, R.V. 2004, "Characterization of the structure of calcium alumino-silicate and calcium fluoro-alumino-silicate glasses by magic angle spinning nuclear magnetic resonance (MAS-NMR)", *Journal of Non-crystalline solids*, vol. 333, pp. 101-107.
- Yue, Y.Z. 2008, "Characteristic temperatures of enthalpy relaxation in glass", *Journal of Non-crystalline solids*, vol. 354, pp. 1112-1118.
- Yue, Y.Z., Christiansen, J.d. & Jensen, S.L. 2002, "Determination of the fictive temperature for a hyperquenched glass", *Chemical Physics Letters*, vol. 357, pp. 20-24.
- Zeng, Q. & Stebbins, J.F. 2000, "Fluoride sites in aluminosilicate glasses: High-resolution ^{19}F NMR results", *American Mineralogist*, vol. 85, pp. 863-867.

B Additional SEM-EDS results

This appendix presents additional SEM-EDS results referred to but not shown in the main thesis. All results are plotted as relative atomic percentages based on a total of ≈ 1200 spot analyses from three images for each sample. The experimental conditions are described in section 4.2.1.

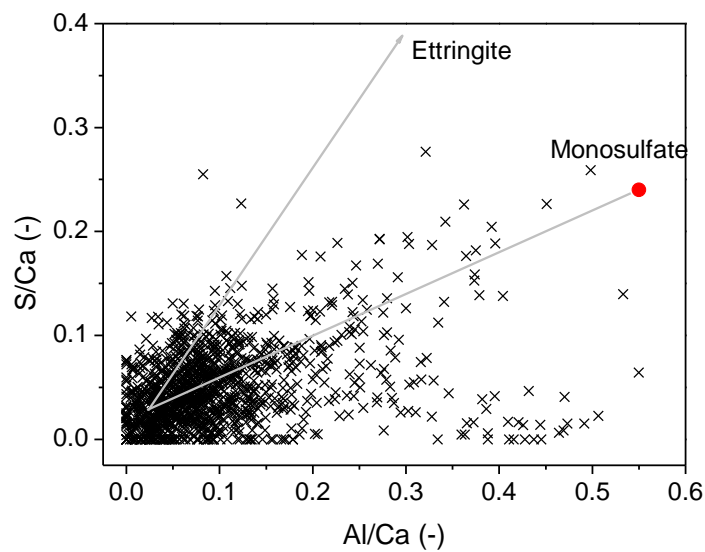


Figure B.1: S/Ca ratios as a function of Al/Ca ratios for EDS spot analyses based on spectral imaging of OPC paste hydrated 90 days.

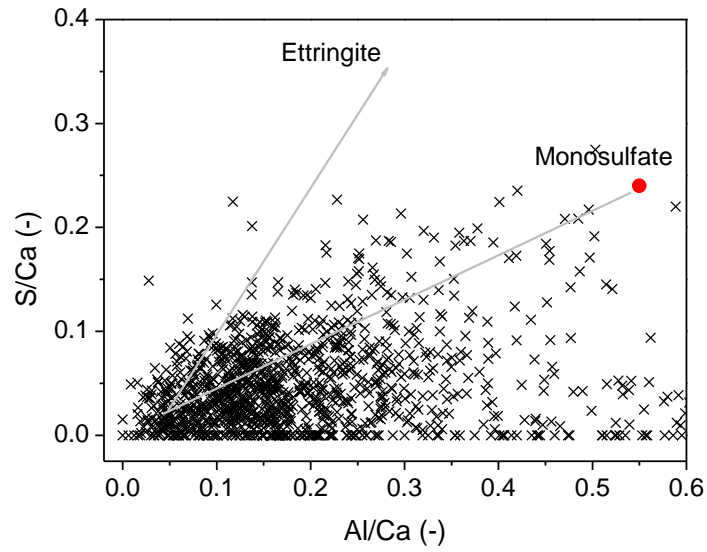


Figure B.2: S/Ca ratios as a function of Al/Ca ratios for EDS spot analyses based on spectral imaging of blended cement paste containing 30 wt% CLS_{9N fine} hydrated 90 days.

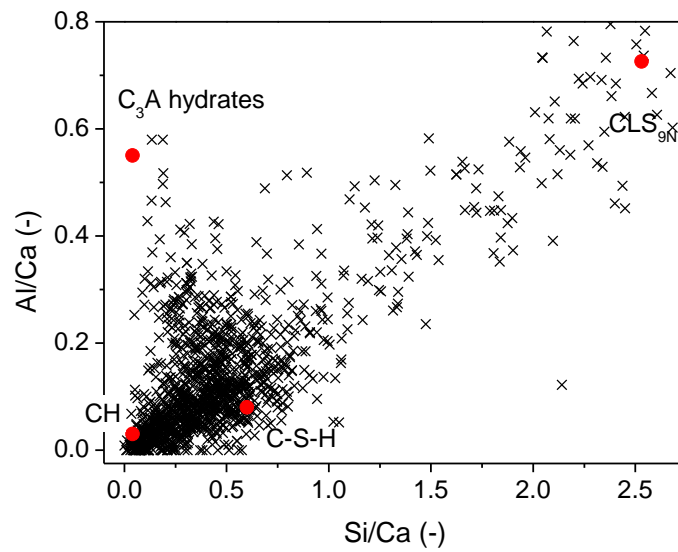


Figure B.3: Al/Ca ratios as a function of Si/Ca ratios for EDS spot analyses based on spectral imaging of blended cement paste containing 30 wt% CLS_{9N fine} hydrated 28 days.

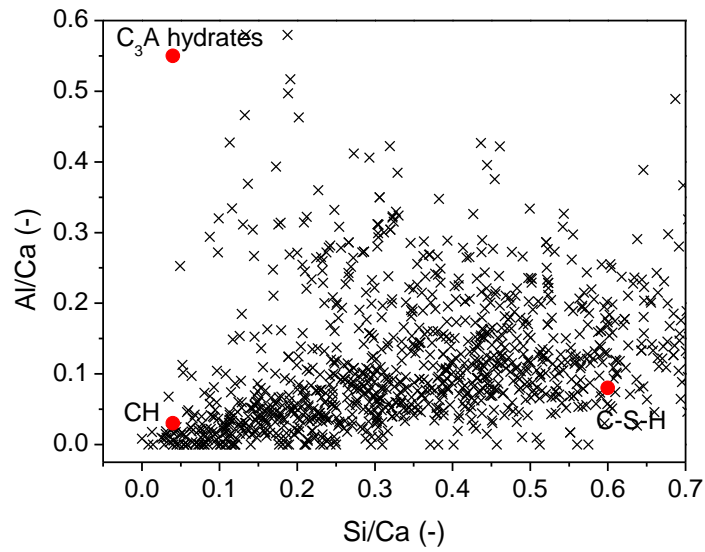


Figure B.4: Al/Ca ratios as a function of Si/Ca ratios for EDS spot analyses based on spectra imaging of blended cement paste containing 30 wt% CLS_{9N fine} hydrated 28 days. The figure shows a zoom on the region of low Al and Si contents.

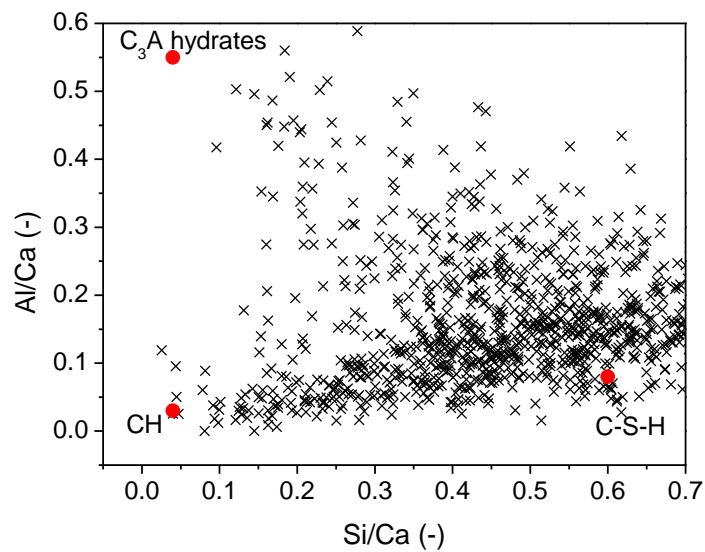


Figure B.5: Al/Ca ratios as a function of Si/Ca ratios for EDS spot analyses based on spectral imaging of blended cement paste containing 30 wt% CLS_{9N fine} hydrated 90 days. The figure shows a zoom on the region of low Al and Si contents.

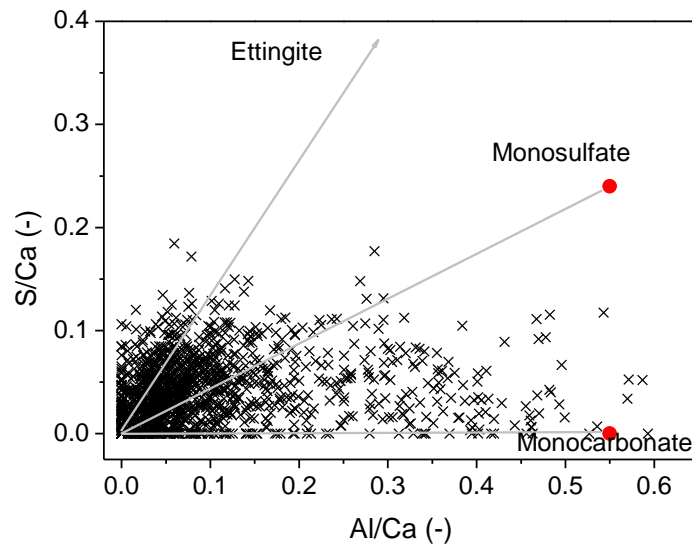


Figure B.6: S/Ca ratios as a function of Al/Ca ratios for EDS spot analyses based on spectral imaging of blended cement paste containing 30 wt% limestone hydrated 90 days.

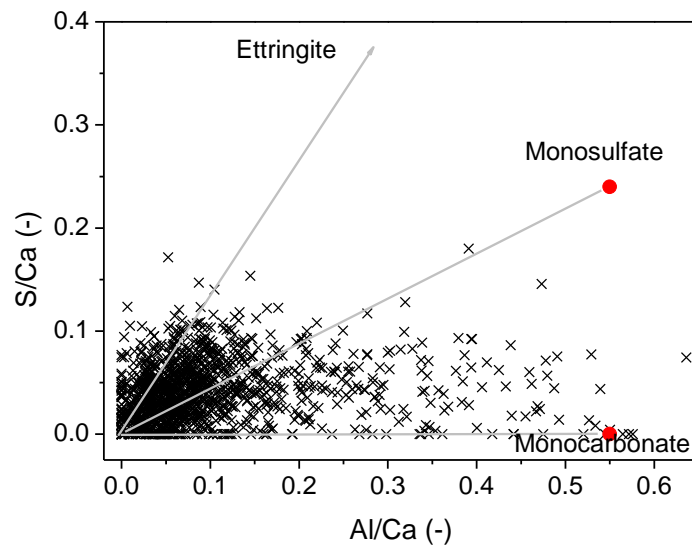


Figure B.7: S/Ca ratios as a function of Al/Ca ratios for EDS spot analyses based on spectral imaging of blended cement paste containing 20 wt% limestone and 10% CLS_{9N} fine hydrated 90 days.

List of publications

I M. Moesgaard, Y. Z. Yue, Compositional dependence of fragility and glass forming ability of calcium aluminosilicate melts, *J. Non-cryst. Sol.*, 355 (2009) 867-873.

II M. Moesgaard, D. Herfort, J. Skibsted, Y. Z. Yue, Calcium aluminosilicate glasses as supplementary cementitious materials, *Eur. J. Glass Sci. Technol. A.*, 5 (2010) in press.

III M. Moesgaard, R. Keding, J. Skibsted, Y. Z. Yue, Evidence of intermediate-range order heterogeneity in calcium aluminosilicate glasses, *Chem. Mater.*, 22 (2010) 4471-4483.

IV M. Moesgaard, D. Herfort, L. F. Kirkegaard, Y. Z. Yue, Optimal composition of calcium aluminosilicate glass particles used as supplementary cementitious materials, Proceedings of the 12th International Inorganic-Bonded Fiber Composites Conference (2010) 23-29.

V M. Moesgaard, D. Herfort, M. Steenberg, L. F. Kirkegaard, Y. Z. Yue, Physical performances of blended cements containing calcium aluminosilicate glass powder and limestone, submitted to *Cem. Concr. Res.*

VI M. Moesgaard, D. Herfort, M. Steenberg, Y. Z. Yue, Mechanical performances of blended Portland cements containing calciumaluminosilicate glass particles, 12th International Inorganic-Bonded Fiber Composites Conference (2010) 30-38.

VII M. Moesgaard, D. Herfort, S. L. Poulsen, J. Skibsted, Y. Z. Yue, Hydration behavior of composite cements containing both calcium aluminosilicate glass powder and limestone, in prep. for *Cem. Concr. Res.*